UNIVERSITY OF CALGARY

Sympathetic Cooling of Gaseous Ions Confined in a Linear Paul Trap

by

Thomas James Harmon

A DISSERTATION

SUBMITTED TO THE FACULTY OF GRADUATE STUDIES

IN PARTIAL FULFILMENT OF THE REQUIREMENTS FOR THE

DEGREE OF MASTER OF SCIENCE

DEPARTMENT OF PHYSICS AND ASTRONOMY

CALGARY, ALBERTA

August, 2003

THE UNIVERSITY OF CALGARY

FACULTY OF GRADUATE STUDIES

The undersigned certify that they have read, and recommended to the Faculty of Graduate Studies for acceptance, a dissertation entitled "Sympathetic Cooling of Gaseous Ions Confined in a Linear Paul Trap" submitted by Thomas James Harmon in partial fulfillment of the requirements for the degree of M.Sc.

Supervisor, Dr. Robert I. Thompson
Department of Physics and Astronomy

NASSER AHMAD

Dr. Nasser Moazzen-Ahmadi
Department of Physics and Astronomy
CO-SUPERVISOR

Dr. David Feder
Department of Physics and Astronomy

Dr. Rene Plume
Department of Physics and Astronomy

Dr. Yujun Shi
Department of Chemistry

August 27, 2003

Date

Abstract

Sympathetic laser cooling of ions stored within a Linear Paul Trap has been investigated using computational and theoretical techniques. The computational simulations, which allow 5 molecular ions to interact with 35 laser cooled atomic ions, revealed an instability heating mechanism which can prevent ions below a certain critical mass from being sympathetically cooled. This critical mass can however be varied by changing the trapping parameters thus allowing ions of any mass to be sympathetically cooled using a single ion species. A theoretical explanation of this instability heating mechanism is presented which predicts that the cooling-heating boundary in trapping parameter space is a line of constant 'q'- the ion trap stability parameter, a result supported by our computational results. In our data, it is also seen that the sample ions do not reach thermal equilibrium with the laser cooled ions, but reach an equilibrium temperature determined by the value of 'q'.

Acknowledgements

Firstly, I would like to thank Dr Robert Thompson, my course instructor and M.Sc. supervisor. As my course instructor, Dr Thompson really brought the strange world of Quantum Mechanics down to earth with a large dose of honesty and realism. While many texts on quantum mechanics suggest an underlying thread of sense to it all, leaving the reader perplexed and confused, Dr Thompson presented quantum theory for what it is. As my course supervisor, Dr Thompson gave me the freedom to think and explore various ideas, some good and some not so good. He also put a lot of faith into me and my abilities, which helped me to develop the good ideas into working theories. Secondly, I wish thank my co-supervisor Nasser Moazzen-Ahmadi for all the hard work and effort he has contributed to my work. During the course of my research, Nasser and myself had many useful and enlightening conversations about molecules. Nasser has also played a critical role in making sure I understood what I was talking about by playing the largely unpopular role of devil's advocate. I would also like to thank the Natural Sciences and Engineering Research Council of Canada and the Faculty of Graduate Studies at the University of Calgary for their financial assistance. D. Hobill and H. Graumann also provided very useful intellectual assistance related to the challenges of computational physics. Finally, I would like to thank the Department of Physics and Astronomy, and Dr Hicks in particular for his help when I was a struggling undergraduate student. The department has provided a very positive and stimulating atmosphere in which to learn and grow, and I am deeply grateful for the opportunity to work with such nice people.

Table of Contents

List of Tables

List of Figures

1. INTRODUCTION

1.1 Laser cooling

Laser cooling [1] has allowed atomic physicists to study gas-phase atomic systems at ultra-low temperatures, largely removing thermal effects and allowing many atomic systems to be studied at their most fundamental quantum level, for example, atom interferometry [2], superfluidity [3] and Bose-Einstein condensation [4]. The reason why these phenomena only exist at such low temperatures can be seen through the de Broglie equation.

$$\lambda = \frac{h}{mu} \qquad (1.1.1)$$

which relates a particle's quantum mechanical wavelength λ to its classical speed u and mass m. This equation asserts that the wavelength of a particle increases as its speed decreases. As the wavelength approaches that of the mean particle spacing, the particles can no longer be treated as localized regions of mass with respect to one another or the container itself, as is done in classical physics, but instead must be treated as broad probability distributions. As such, the collisions between the particles themselves and the collisions between the particles and walls of the container must also be treated

probabilistically. The equation that propagates these wavefuctions is the Schrodinger Equation. At low temperatures atoms can be made to interfere like ordinary waves, and can also behave like a superfluid by virtue of a linear dispersion relationship[1] that arises from the coupling between atoms [5]. Bose-Einstein condensation occurs when Bosonic atoms are forced into the ground state of the system. In the ground state, the particles all share the same phase and are thus coherent. The wave-like nature of matter can be demonstrated by colliding two condensates and observing the interference fringes they produce. Although a range of neutral and ionic atomic systems have been cooled to sub-Kelvin temperatures with direct laser cooling[2], there is a limitation to this approach.

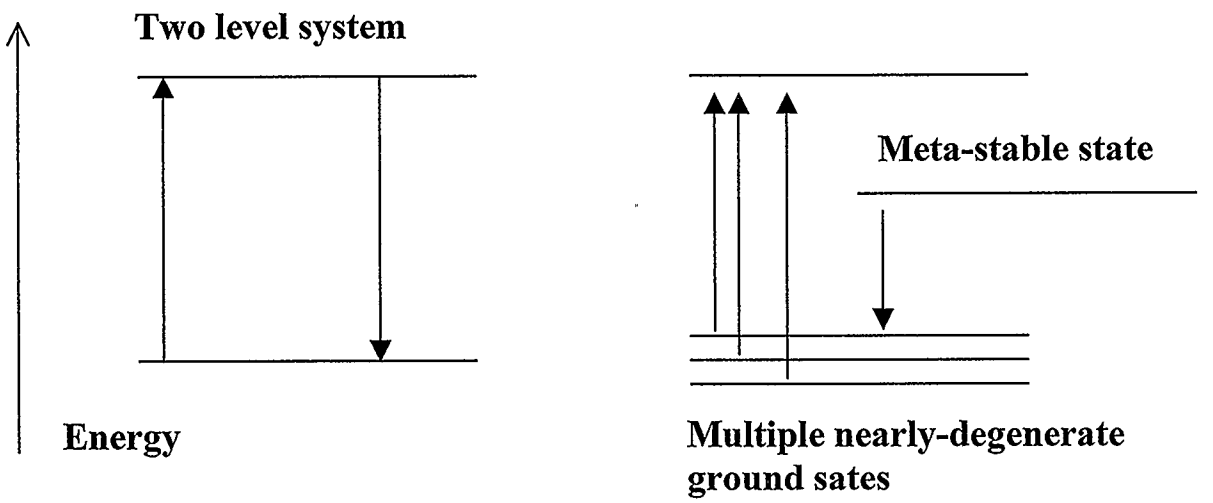

Fig. 1.1.1. Energy level diagram for a two level system requiring one pumping laser, and a multiple level system requiring an additional re-pumping laser for each level.

[1] This is only true for homogeneous gases.

[2] There are many excellent papers and books on laser cooling such as those in [1]. Briefly, Laser Cooling a.k.a.Doppler Cooling, uses the absorption of single photons to reduce an atoms speed. The photons are deliberately red shifted so as to only be absorbed by atoms moving towards the laser beam, but then scattered in random directions through spontaneous emission. The net effect is a slowing down of the atom. This process only works on a two level system since many cycles of the above process are required.

Conventional laser cooling techniques, both Doppler [6] and sub-Doppler [7], require isolated two- or three-level systems (see Figure 1.1.1). If a system has additional low-energy meta-stable states or multiple nearly degenerate ground states (e.g. rotational structure in molecular ions) then the laser-cooling cycle terminates when the system falls into a non-resonant level. The solution to this problem generally requires one additional re-pumping laser system for each meta-stable state (e.g. Ref. [8]). Cooling of molecules is especially challenging due to their large number of accessible rotational states. Understandably, there only exists a small number of very complicated theoretical proposals (e.g. Ref. [9]) to directly cool molecular ions.

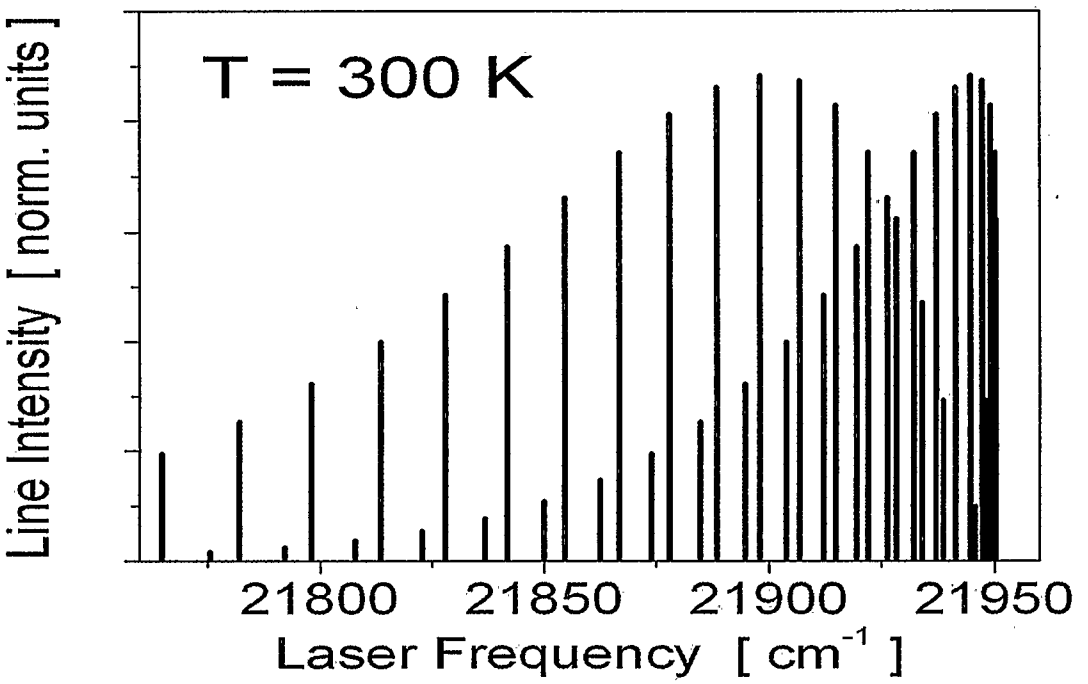

Fig. 1.1.2. A theoretical plot of line intensity vs frequency for CO^+ at 300 K. The spectrum at 300 K has many low intensity lines because population is spread out over many levels.

One of the aims of our research at the University of Calgary is to carry out high resolution spectroscopy on molecular ions. To do this, the ions must not only be translationally cool, but also internally cool. Such internally cool molecular ions, by virtue of the increased population of the lower energy levels, would render a much more intense and less cluttered absorption spectrum than would otherwise be observed at higher temperatures. Figure 1.1.2 shows a theoretical spectrum of CO^+ at 300K. In this plot we see a number of lines due to the presence of a broad population distribution with respect to the energy levels. Compare this with Fig. 1.1.3, a theoretical spectrum of CO^+ at 10K, here we see a few intense lines that can more easily be assigned to their

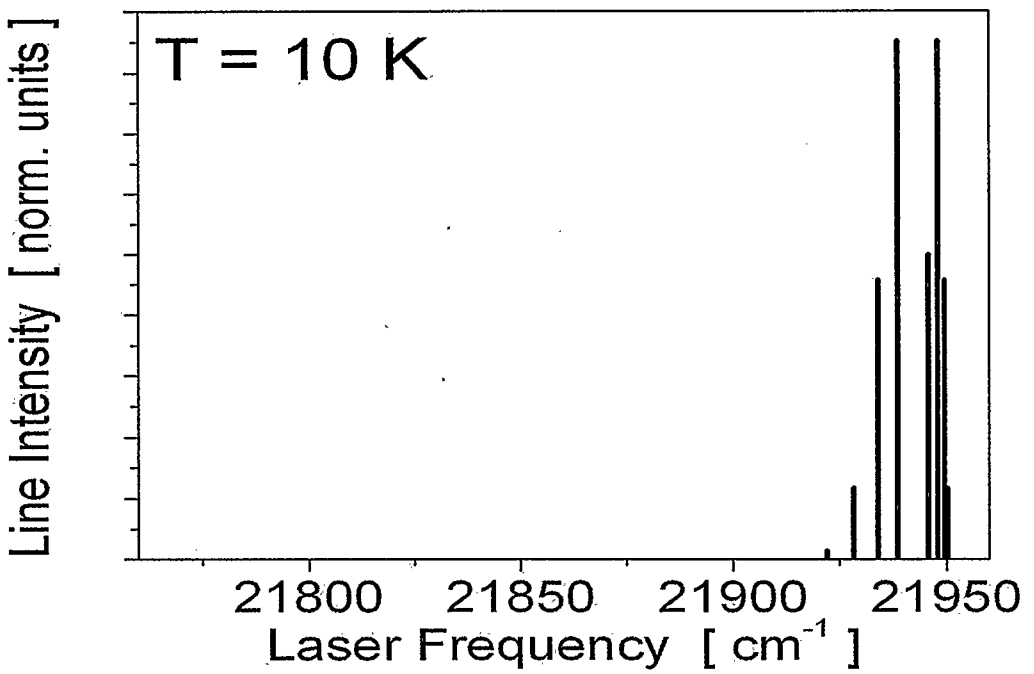

Fig.1.1.3. A theoretical plot of line intensity vs frequency for CO^+ at 10 K. The spectrum exhibits only a few intense lines because the population is limited to the lower energy states.

It is yet to be determined whether or not molecular ions would cool internally (vibrationally/rotationally) through translational cooling in an ion trap, but it seems like a logical first step to first slow the molecules down. This would also have the effect of reducing the spectral line width thus increasing the resolution and intensity of the spectrum. Unfortunately, many atomic systems, i.e. those lacking the necessary energy level structure, and virtually all molecular systems cannot be directly laser cooled. However, a much wider range of atomic and molecular systems can be taken to very low temperatures through a process known as sympathetic cooling [10].

1.2 Sympathetic cooling

In this technique, a collection of two interacting species, the sample species (which can not be directly laser cooled) and the laser-cooled species, are confined to the same region of space and isolated from their surroundings through the use of neutral particle or ion traps. As the laser-cooled species interacts with the light field its temperature falls. When these cold atoms interact or collide with the sample species, they extract energy from the sample species, sympathetically reducing the sample species temperature. Recently, a variation on this approach has been applied to neutrals whereby evaporatively-cooled atoms sympathetically cool a sample species to produce Quantum Degenerate Gases from species whose self-interaction (the interaction between one atom with another identical atom) is too weak to permit efficient evaporative cooling on its own [11]. This type of sympathetic cooling in neutrals depends fundamentally on the

short range interactions (collisions) between the directly-cooled and sample species, and thus the effectiveness of sympathetic cooling depends fundamentally on the particular pair of species selected and their associated inter-atomic or atom-molecule interaction potentials. This makes it rather difficult to produce simple and broadly general rules regarding the effectiveness of sympathetic laser cooling that would apply to all neutral atomic and molecular species. However, when considering sympathetic cooling between ions, the dominant interaction force is Coulomb interactions, which are both long range and quite strong. This means that ions do not tend to approach each other closely enough to probe the short-range interaction potentials that differ from atom to atom and molecule to molecule. Therefore, the effectiveness of sympathetic cooling between charged particles tends to be a function of only the mass and charge-state of each of the two ions, allowing for rather generalized rules regarding sympathetic cooling of charged particles to be deduced.

1.3 Previous research on sympathetic cooling

This thesis work marks the beginning of a theoretical and experimental program at the University of Calgary to study the processes associated with the sympathetic cooling of ions. The long term goals of this project are to develop the tools and expertise to produce low-temperature, gas-phase samples in as wide a range of atomic and molecular species as is physically possible for use in such areas as molecular spectroscopy, spectroscopy of stable and unstable atomic isotopes, and the physical implementation of Quantum

Information Science protocols. The following pages outline a computational/theoretical study of the apparently simple questions: Firstly, what is the range of ion masses that a particular laser cooled ionic species can sympathetically cool in a quadrupole ion trap, and secondly, to what limiting temperature can one sympathetically cool these ions ?

Sympathetic cooling of molecular ions by laser-cooled atomic ions within a linear Paul trap has been experimentally demonstrated [12] using ions of similar mass; reaching translational temperatures below 100 mK. Further experimental and molecular dynamics (MD) computational simulations have shown axial translational temperatures as low as 10 mK using a single ion species to sympathetically cool over a wider mass range [13], but no particular or general limits on this range were determined. More recently, work related to a novel ion trap in-situ mass spectrometry technique under development by Baba and Waki [14] has lead to an MD simulation study, which illustrated that for particular trap conditions there is a lower bound on the sample ion mass (m_s) that can be sympathetically cooled. This limit is quoted as 0.54 times the mass of the laser cooled ion (m_c) [15]. However, no upper bound on the masses that could be sympathetically cooled was examined. My work investigates the cooling of higher mass ions, confirming the lack of a concrete upper bound, and examines the question of sympathetic cooling of light sample ions in a more general setting. The latter point revealed techniques to modify the cooling threshold value, and provided a general theoretical framework for the heating processes in terms of the concept of instability heating. This work also investigates not only under what conditions cooling occurs, but also the limiting temperature of the cooled sample ions.

2. SYMPATHETIC COOLING OF TRAPPED IONS[3]

2.1 Single ion motion in a linear Paul Trap

As mentioned in the previous section, sympathetic cooling of ions operates through Coulomb interactions with laser cooled ions. Theoretically, such interactions between ions that are completely isolated from their surroundings will eventually bring all of the ions into thermal equilibrium. If the ions interact only with laser cooled ions kept at a constant temperature, all of the ions should then come into thermal equilibrium at the fixed temperature of the laser cooled ions. However, trapped ions are not in fact completely isolated because the electric (and magnetic for Penning Traps) fields used to suspend the ions in space can themselves produce a number of heating mechanisms (e.g. RF heating [16]) and it is the balance of laser cooling and trap heating that leads to an equilibrium temperature. Therefore, depending on the relative efficiency of energy extraction through collisions with laser cooled ions and trap-related heating effects a given ion can either increase or decrease its energy. It is this balance that leads to the heating-cooling threshold observed in Ref. [15]. This work will concentrate on ions stored in a linear-geometry, RF quadrupole-electric field trap (commonly referred to as a linear Paul trap). In this type of trap, the ions are contained in the z-direction by a DC trapping field, while a RF-oscillating saddle-shaped potential traps the ions in the xy-plane [17].

---

[3] The next three chapters are a modified version my previously published work [18].

The stability of a single charged particle in an oscillating electric quadrupole field is discussed in many references [17,19,20]. Highlighting the relevant points, we start with a single ion in a linear Paul Trap, where the confining potential along the z-axis of the quadrupole is approximated as harmonic. The ion is subject to the following potential in x and y coordinates:

$$\Phi(x,y) = \frac{U_{rf}(y^2 - x^2)\cos(\Omega t)}{2r_0^2}, \tag{2.1.1}$$

where U_{rf} and Ω are the amplitude and angular frequency of the applied rf-electric trapping potential, respectively, while r_o is the distance from trap centre to one of the electrodes. Given that $\mathbf{F} = -e\nabla\Phi$, the equations of motion for the ion of mass m and charge e in the xy plane are given by:

$$\begin{aligned} \ddot{x} + (e/mr_0^2)(U_{rf}\cos\Omega t)x = 0, \\ \ddot{y} - (e/mr_0^2)(U_{rf}\cos\Omega t)y = 0. \end{aligned} \tag{2.1.2}$$

Recasting these equations using the unitless parameters $\xi = \Omega t/2$ and

$q_u = q_x = -q_y = 2eU_{rf}/m\Omega^2 r_0^2$ produces

$$\frac{\partial^2 u}{d\xi^2} - (2q_u \cos 2\xi)u = 0, \qquad (2.1.3)$$

where u represents either x or y. Equation (2.1.3) is the Mathieu equation in its canonical form [21], its general solution being

$$u = \alpha' e^{\mu\xi} \sum_{n=-\infty}^{\infty} C_{2n} e^{2in\xi} + \alpha'' e^{-\mu\xi} \sum_{n=-\infty}^{\infty} C_{2n} e^{-2in\xi} \qquad (2.1.4)$$

where α' and α'' are integration constants determined by the initial conditions, (i.e. $u(\xi_o)$, $\dot{u}(\xi_o)$ and ξ_o), while C_{2n} and μ depend solely on the value of q_u and not the initial conditions [20]. If μ is purely imaginary then the ion will have an oscillatory motion (trapped particle). However, if μ is real or complex the motion will be unbound (unstable particle). The determination of μ from q_u in general is a difficult problem and is best handled numerically. It is well established in the literature [17] that if $|q_u| < 0.908$, then μ is purely imaginary and if $|q_u| > 0.908$ the parameter μ then becomes complex, other than for some very localized values of q_u. For this reason q_u is called the stability parameter. The effect of q_u being less than or greater than 0.908 is illustrated in Figs. 2.1.1 and 2.1.2. For stable trapping parameters, the motion of an ion in x and y, as described by Eq. (2.1.4), can be broken down into a superposition of the ion's micromotion and its secular motion. The micromotion is an oscillatory motion at the angular frequency of the

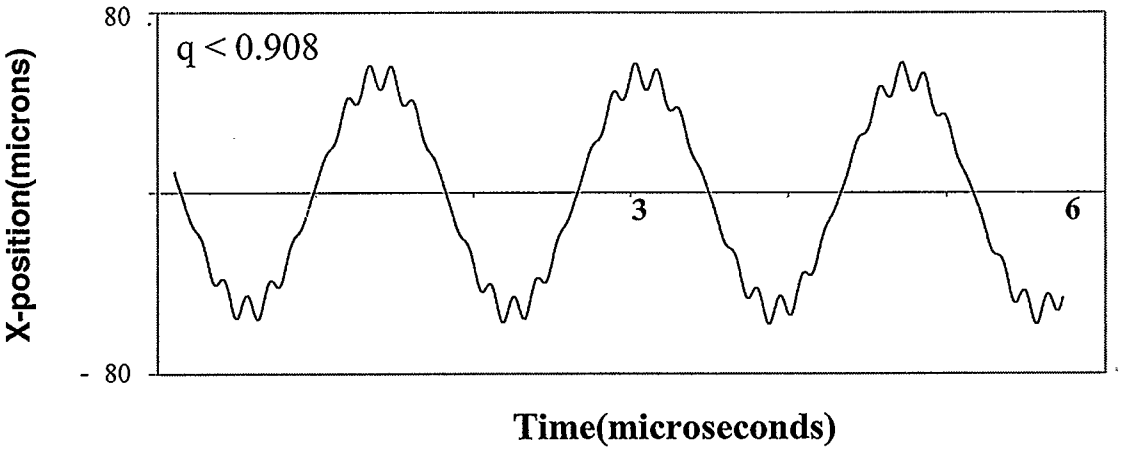

Fig. 2.1.1. A plot of x-position vs time showing bounded ion motion when q < 0.908. The low frequency oscillation is called secular motion. The higher frequency oscillation superimposed on the secular motion is called micromotion.

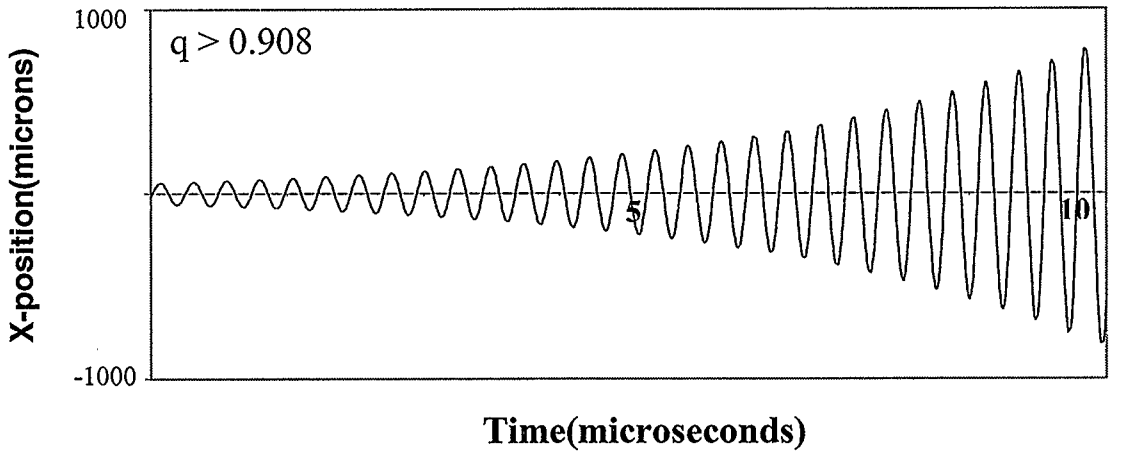

Fig. 2.1.2. A plot of x-position vs time showing unbounded ion motion when q > 0.908.

trapping field that increases in amplitude the further the ion is from the trap centre. It is the direct result of the oscillation of the trapping field driving the ion back and forth as the field reverses. The secular motion, which for trapped particles has a lower frequency

than the micromotion, is a simple harmonic oscillation in the time-averaged pseudo-potential generated by the trapping field. The secular frequency of this motion, for small values of q_u, is given by [20]:

$$\omega_{sec} = \frac{q_u}{\sqrt{8}}\Omega, \tag{2.1.5}$$

while the amplitude can be expressed in terms of the temperature based on the assumption[4] of ½ $k_B T$ of energy in the relevant mode:

$$u_0 = \frac{1}{q_u \Omega}\sqrt{\frac{16 k_B T}{m}}. \tag{2.1.6}$$

Here u_0 is the amplitude of motion, k_B the Boltzmann constant, and m the ion mass.

2.2 Computer simulation of multiple ions in a Linear Paul Trap

Sympathetic cooling requires that multiple interacting ions are simultaneously stored in the trap. We cannot deal with such a many-body system analytically, but rather it is possible to calculate the motion of each ion by integrating the equations of motion for each ion in the trap. Additional terms have to be added to Eq. (2.1.2) to account for the Coulomb repulsion between each of the ions, as well as the laser cooling [22]. The

[4] This was computationally verified by both Baba and Waki [15] and myself. See end of section 2.2

equation of motion for z is similar to the x and y equations, although it is simpler because the electric field in this direction is static and harmonic, centered at the trap center. The 0.025 below corresponds to the center of the 5 cm long central trapping electrodes[5].

$$\phi(z) = C(z - 0.025)^2 \qquad (2.2.1)$$

The simulation numerically integrated the motion of 35 laser cooled Mg^+ ions interacting with 5 sample ions using the Euler-Picard predictor-corrector method with 0.1 to 1 ns time-steps (see Appendix A). The ions were confined radially by the potential given by Eq. (2.1.1). and axially by a harmonic potential with a force constant of 1 mV/mm. The initial conditions for the simulations started the ions in random positions with the sample ions at a temperature of 40 K and the laser cooled ions at a temperature of 15 K. The laser intensity was selected so that in the absence of sample ions, the heating balanced the laser cooling and the laser-cooled ion temperature would not further reduce. In addition, the laser intensity was maintained at a low enough level to prevent the formation of ion crystals[6] [23,24,25]. These conditions were chosen to be equivalent to those used in Ref. [15]. The simulation output provided the average sample ion and laser cooled ion temperature as a function of time. The temperature was calculated by taking the average

[5] It should be noted that the form of the potential generated by the electrodes is more like a square well [26] potential when the ion temperature is above 1 K. However, the potential in this direction really only affects the collision rate between the ions as they bounce back and forth up the trap. Therefore we modeled the z potential as a steep harmonic well to increase the collision rate and thus save computational time.

[6] At low enough temperatures the ions have insufficient kinetic energy to overcome the interionic potential and pass each other. This localizes them in space, forming an ion or Wigner crystal.

energy of each ion over 4 cycles of secular motion and then calculating the average ion energy for the five sample ions and the thirty five laser-cooled ions, independently. The ion temperatures were determined from these average energies using [15]

$$\langle E \rangle_t = \frac{5}{2} k_B T . \qquad (2.2.2)$$

The factor of 5 in Eq. (2.2.2) takes into account the fact that we have 5 energy storage modes. The ion's secular motion oscillates harmonically in both the x and y directions, and the ion also oscillates harmonically in the static harmonic potential along the z direction. These three contributions add giving 3/2 kT to the mean kinetic energy. The important point to note about the ion's oscillatory motion in the x and y directions, is that since the ion is not confined by a static harmonic potential, the ½ kT of energy that would be associated with the potential energy, is actually transferred into micromotion instead, decreasing the heat capacity. Since the micromotion is kinetic energy, we must add the extra ½ kT from the micromotion in both the x and y directions to the total kinetic energy. This gives us a total kinetic energy of 5/2 kT.

2.3 Simulation results

Integration was generally carried out for 30 ms, which was usually sufficient to determine whether the temperature of the sample ions was increasing or decreasing with time. First,

the laser-cooled ions were interacted with a range of more massive sample ions (up to 8 times the mass of the laser-cooled ions, m_c). This confirmed that those sample ions heavier than the laser-cooled ions generally cooled. However, as the mass difference increased, the rate of cooling decreased. Next, the case in which the sample ions are less massive than the laser-cooled ions was examined. For a given U_{rf} and Ω, heating or cooling of the sample ion was observed to depend on its mass, m_s. We confirmed that for the same trap conditions as in Ref. (15), there is the same lower bound on the sample ion mass that can be sympathetically cooled, i.e. $m_s = 0.54m_c$.

Since heating is thought to involve energy transfer from the trapping fields, at this point, tests were made to determine if sample ions with $m_s < 0.54m_c$ could be cooled by changing the trap parameters. It was found that there always exist values of q_u for which this is possible. A large number of simulations for a range of sample ions with mass below $0.54m_c$ were carried out. In all cases the results were more or less the same as those illustrated in Figs. 2.3.1 and 2.3.2. Figure 2.3.1 is for $m_s = 8$ amu and Fig. 2.3.2 is for $m_s = 12$ amu, while $m_c = 24$ amu in both cases. Both of these figures show the typical result that if the value of q_u is reduced sufficiently, the sample ions can be cooled. To further test this hypothesis, maps of the U_{rf}-Ω space were made to determine the trapping field parameters for which the sample ions heated, cooled, or remained basically unchanged in temperature. Figures 2.3.3 and 2.3.4 show a pair of typical maps.

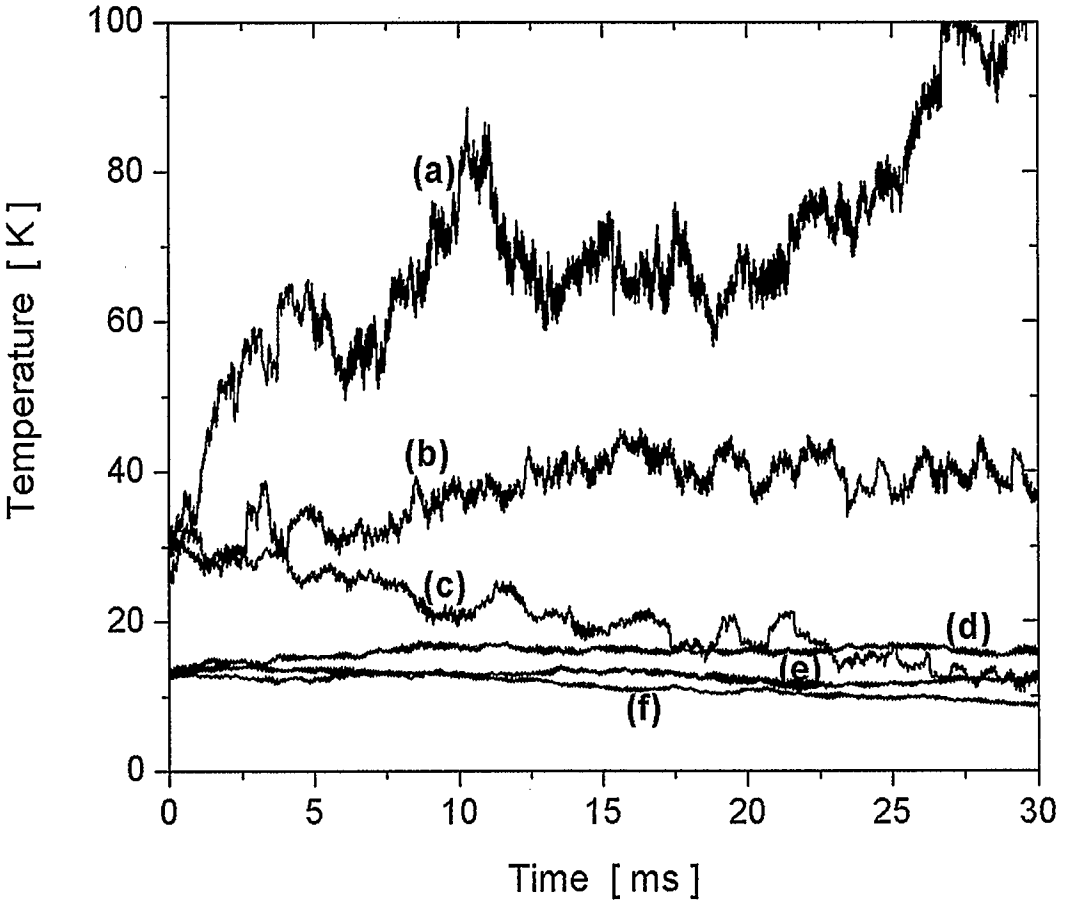

Fig. 2.3.1. Temporal plots of the average temperature (see text) of 8 amu sample ions and 24 amu laser-cooled ions stored in a linear Paul trap calculated under three different trapping conditions. Line (a) is the sample ion temperatures for $U_{RF} = 50$ V, $\Omega = 2\pi(2.5$ MHz), and $q_u = 0.71$; line (b) is the sample ion temperatures for $U_{RF} = 100$ V, $\Omega = 2\pi(4.5$ MHz), and $q_u = 0.53$; line (c) is the sample ion temperatures for $U_{RF} = 30$ V, $\Omega = 2\pi(2.75$ MHz), and $q_u = 0.35$. Lines (d), (e), and (f) are the laser-cooled ion temperatures corresponding to the conditions for (a), (b), and (c), respectively.

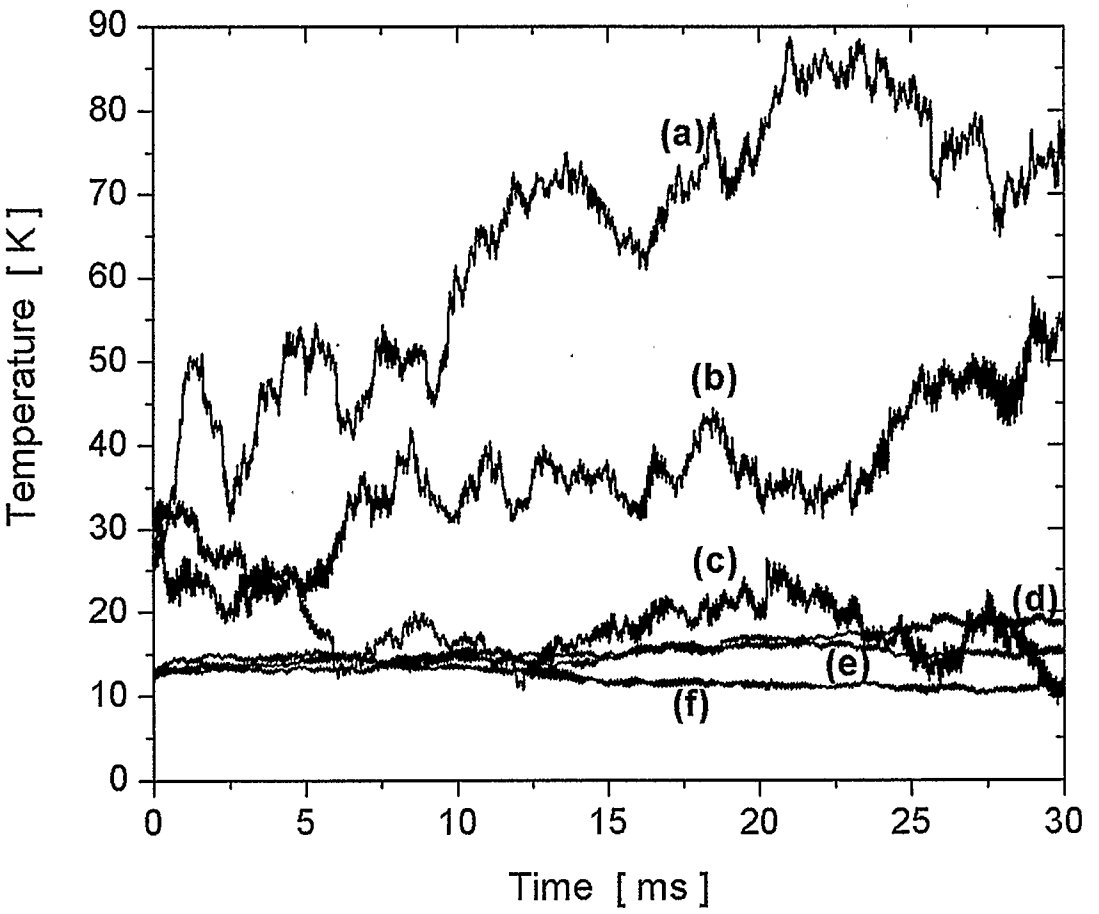

Fig. 2.3.2. Temporal plots of the average temperature (see text) of 12 amu sample ions and 24 amu laser-cooled ions stored in a linear Paul trap calculated under three different trapping conditions. Line (a) is the sample ion temperatures for U_{RF} = 40 V, $\Omega = 2\pi$(2 MHz), and q_u = 0.59; line (b) is the sample ion temperatures for U_{RF} = 70 V, $\Omega = 2\pi$(2.6 MHz), and q_u = 0.61; line (c) is the sample ion temperatures for U_{RF} = 40 V, $\Omega = 2\pi$(2.5 MHz), and q = 0.35. Lines (d), (e), and (f) are the laser-cooled ion temperatures corresponding to the conditions for (a), (b), and (c), respectively.

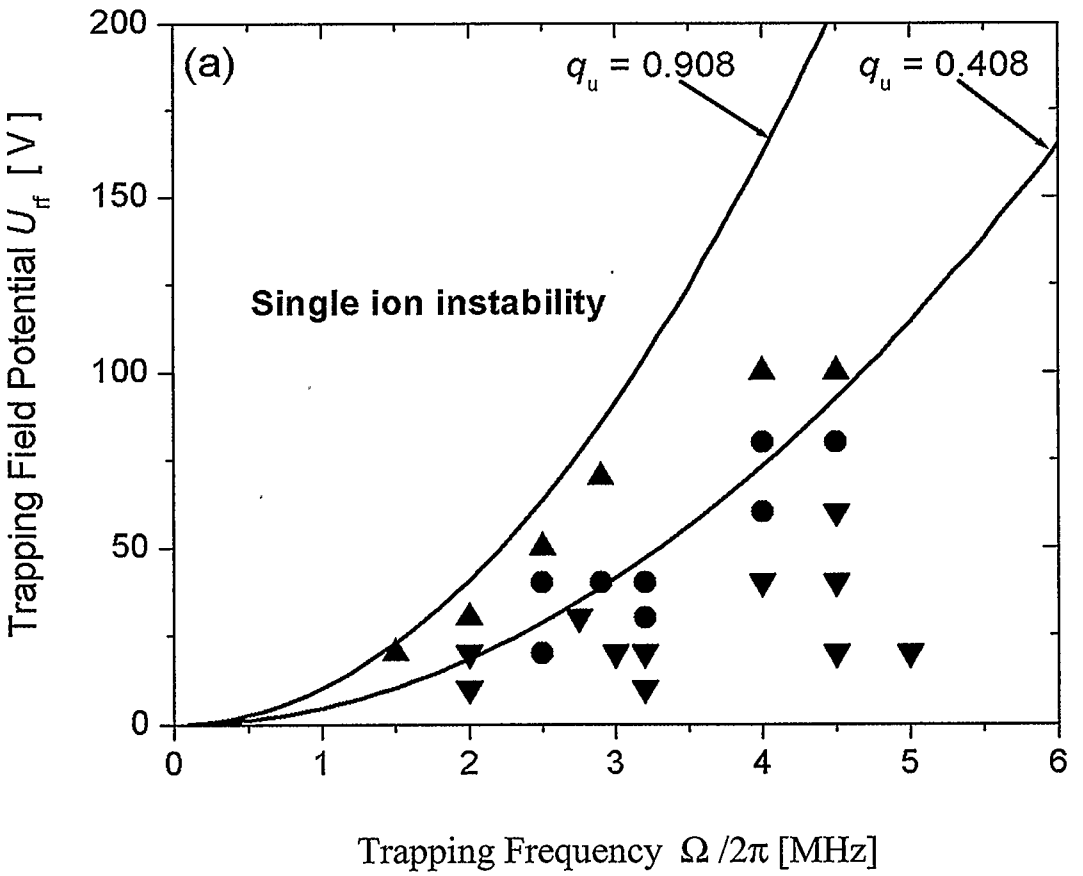

Fig. 2.3.3. Maps of the regions of heating and cooling in $U_{RF} - \Omega$ space for 5 sample ions and 35 laser-cooled ions in a linear-geometry Paul trap. ▲ indicates simulations that produced ion heating, ▼ indicates ion cooling, and ● indicates no definitive change in temperature. Plot (a) is for 8 amu sample ions and 24 amu laser cooled ions. The solid line indicates the $q_u = 0.908$ stability threshold for single ion trapping, while the second constant q_u line in each figure is the theoretical threshold between regions of sympathetic cooling and heating of the sample ions (see text).

The $q_u = 0.908$ curve indicates the single sample ion trapping stability threshold. As can clearly be seen, sympathetic cooling does not occur close to this threshold and thus the ions are heated. As we move away from this threshold we reach a region where there

appears to be a balance and the ions neither heat nor cool. Finally, for low enough values of q_u sympathetic cooling begins to occur. The questions that now need to be addressed are: What is the physical source for this heating-cooling threshold and can its shape and location be predicted ?

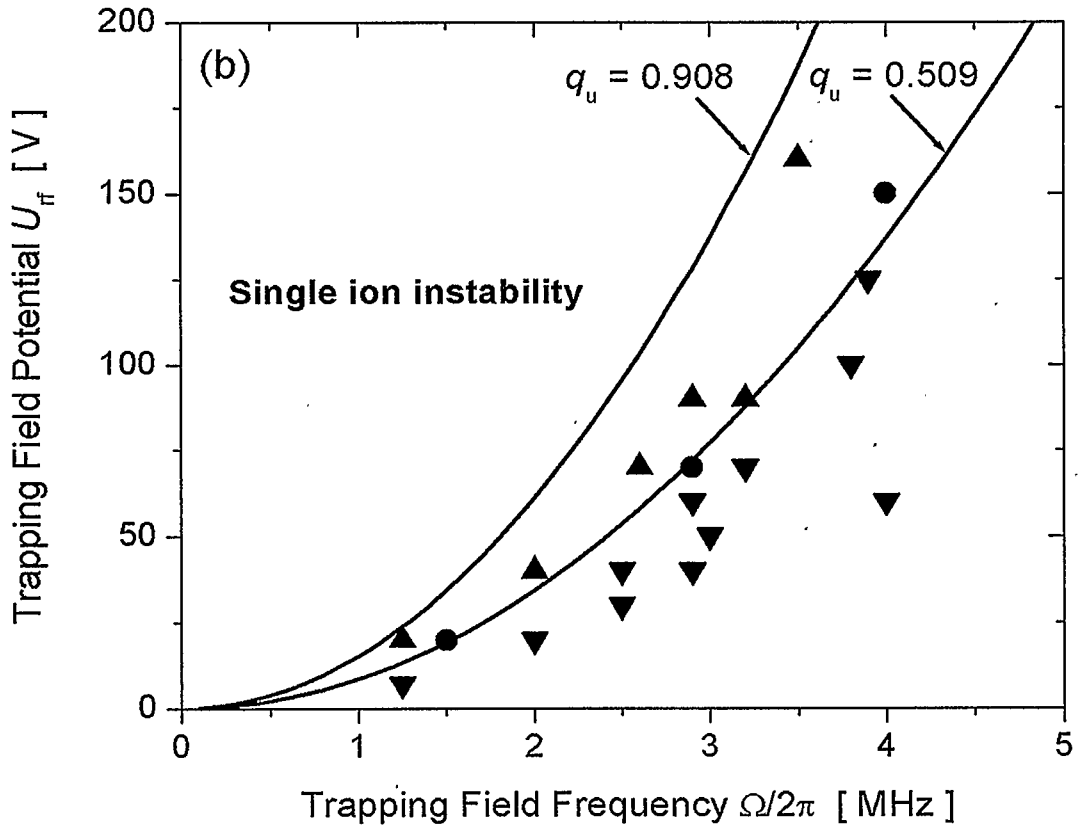

Fig. 2.3.4. Maps of the regions of heating and cooling in $U_{RF} - \Omega$ space for 5 sample ions and 35 laser-cooled ions in a linear-geometry Paul trap. ▲ indicates simulations that produced ion heating, ▼indicates ion cooling, and • indicates no definitive change in temperature. This plot is for 12 amu sample ions and 24 amu laser cooled ions. The solid line indicates the q_u = 0.908 stability threshold for single ion trapping, while the second constant q_u line in each figure is the theoretical threshold between regions of sympathetic cooling and heating of the sample ions (see text).

3. INSTABILITY HEATING THEORY

3.1 The effective instability parameter

Although we have not yet discussed the precise heating mechanism responsible, the results summarised in Figs. 2.3.3 and 2.3.4. clearly suggest the existence of a second mass threshold for the behaviour of trapped ions. The first mass threshold, dictated by the $|q_u| < 0.908$ trap stability criterion, determines if the ion stays in the trap. The second higher-mass threshold (lower q_u), which is also a function of the trapping field parameters, determines whether or not the sample ion can be sympathetically cooled.

From the results of the previous section, it is reasonable to conclude that the two mass thresholds have similar functional dependences on the trapping field parameters and ion mass, suggesting that the physical causes of these two thresholds might be related. This consideration lead us to investigate if the heating process is related to transient instabilities in the ion motion due to interactions with the other ions in the trap, an effect not considered in the single ion trapping model. We will refer to this process as instability heating.

The basic physical mechanism for instability heating is as follows. Equation. (2.1.4) gives the general form for ion motion in an oscillating quadrupole field. For a single trapped ion, q_u is a constant and for $|q_u|$ lower than 0.908, μ is purely imaginary, thus the orbit is oscillatory. When $|q_u| > 0.908$, μ will contain a real part which will cause

the displacement of the ion from the trap centre to grow exponentially. This will in turn cause the ion energy to increase since the energy is proportional to the square of the ion amplitude. However, when the ion in question is in the presence of other ions, q_u can no longer be considered a constant but the additional randomly varying Coulomb forces require it to be replaced with a time-varying effective stability parameter $q_{eff,u}$. Viewed as such, $|q_{eff,u}|$ can now exceed the threshold value of 0.908 for short periods of times without the ion escaping the trap. These time intervals in which the ion trajectory grows exponentially are followed by longer intervals for which $|q_{eff,u}|$ drops below 0.908 thus

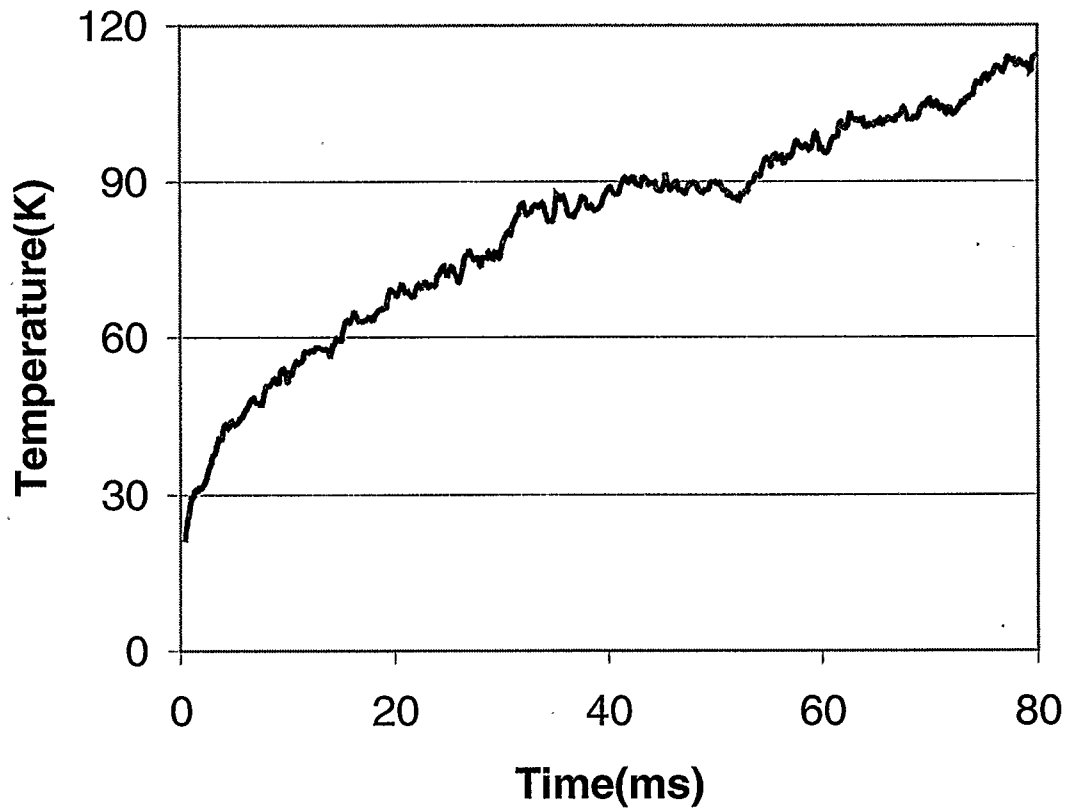

Fig. 3.1.1. Ion Temperature vs Time. As the ions temperature increases, the ion density decreases, reducing the heating rate. This helps prevents the ions from being expelled.

re-stabilizing the ion at a larger maximum radius and a higher energy orbit. As the radius of the ions increases, the overall volume of space in which the ions are trapped increases, decreasing the ion density. Since the collision rate is proportional to the density, the heating rate drops as the temperature increases (see Fig. 3.1.1.). This is one reason why the ions are not expelled from the trap. The other reason, that will be discussed in detail in section 4.1, is that the heating process itself becomes less effective as the ion temperature increases.

To calculate $q_{eff,u}$, we will consider our physical system at a particular point in time and model the sample ion of interest, which is exposed to the trap forces ($F_{T,u}$) and Coulomb force due to other ions ($F_{i,u}$) present in the trap, with an equivalent ion. Furthermore, we will assume that this equivalent ion is positioned at the same point in the trap as the ion of interest, having the same velocity and acceleration, and is subject to the same trap force but is not exposed to the Coulomb force due to the other ions, thus requiring it to have a time-varying effective mass. The effective mass of the equivalent ion in terms of the mass of the sample ion is given by

$$m_{eff,u} = \frac{m}{(1 + \frac{F_{i,u}}{F_{T,u}})}. \qquad (3.1.1)$$

Since the effective mass is the mass for an equivalent single ion in a trap, Eq. (3.1.1) can now be used to obtain $q_{eff,u}$ given by

$$q_{eff,u}=q_u(1+\varepsilon_u), \tag{3.1.2}$$

where

$$\varepsilon_u=\frac{F_{i,u}}{F_{T,u}}. \tag{3.1.3}$$

Note that $q_{eff,u}$ is both time varying and can also have different values in the x and y directions. We can now write the instantaneous stability criterion as

$$\left|q_{eff,u}\right|=\left|q_u(1+\varepsilon_u)\right|\leq 0.908. \tag{3.1.4}$$

When $|q_{eff,u}| > 0.908$ (i.e. when the inter-ionic forces sufficiently exceed the trapping forces) we would expect the possibility of exponential growth of ion trajectory, leading to increased ion temperatures. Figures 3.1.2a and 3.1.2b illustrate that this is indeed the case. These simulations show a short snapshot of the temporal evolution of the x-coordinate of a sample ion in parallel with the computed value of $q_{eff,x}$. They were obtained with a single sample ion and a single laser-cooled ion to clarify the effect, with q_u (= 0.9) set very near the single ion instability threshold in order to maximize the frequency of instability points. The evolution of the particle motion shows a sequence of

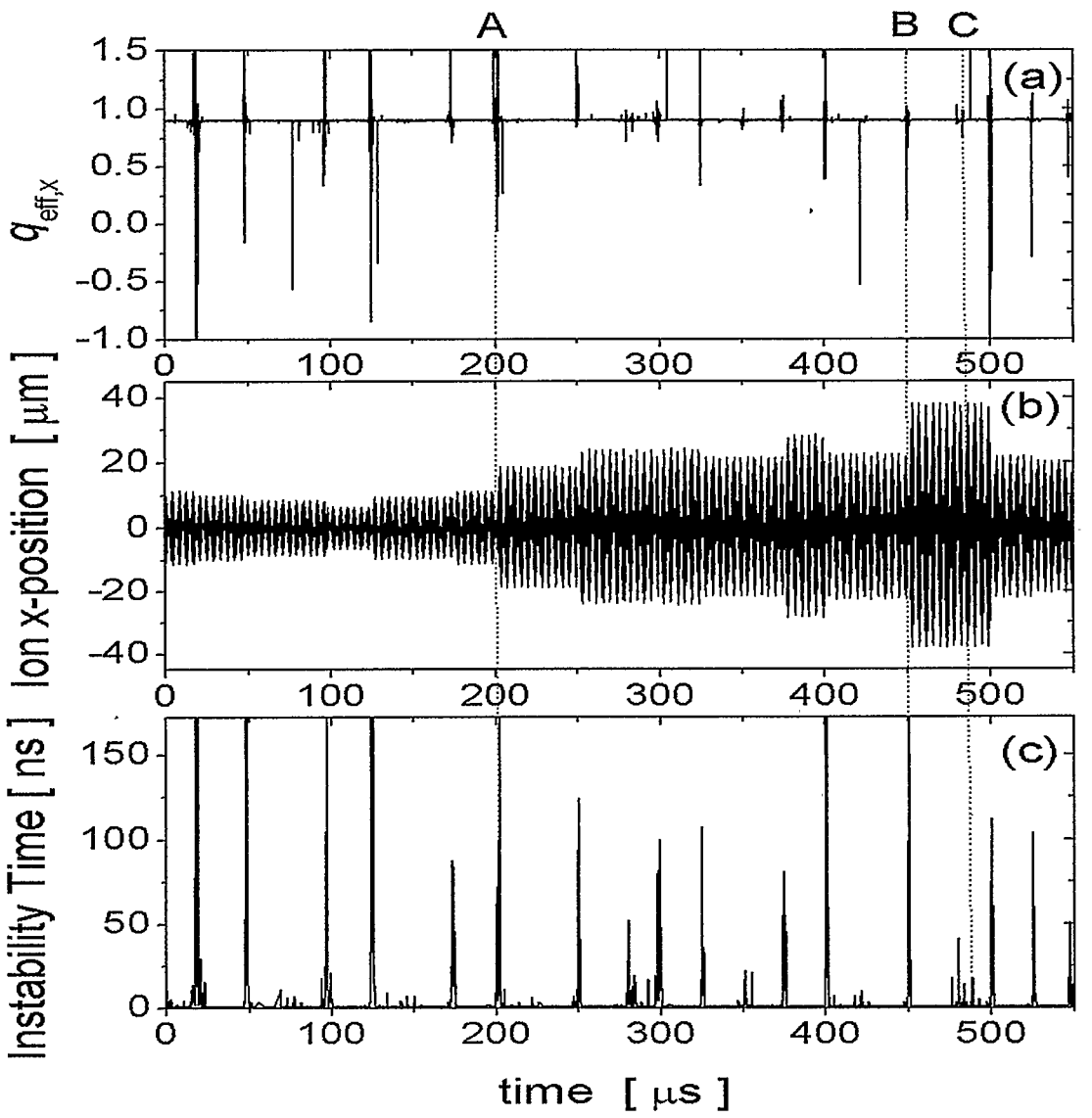

Fig. 3.1.2. Temporal plots of the computed evolution of (a) $q_{eff,x}$ (see text), (b) the x-position and (c) the time period that $q_{eff,x}$ remained above 0.908 for the sample ion in a simulation involving a 6.6 amu sample ion and a 30 amu laser-cooled ion. The trapping field parameters were $U_{RF} = 70V$, $\Omega = 2\pi(2.9\ MHz)$, and $q_u = 0.9$.

steps in the amplitude of the ion's motion, corresponding to steps in the temperature of the ion. For each of these steps, we observe a corresponding spike in $q_{eff,x}$ where $|q_{eff,x}|$ exceeds 1. In some cases, the amplitude steps down instead of increasing, which is expected since Eq. (2.1.4) contains both exponentially growing and decaying terms. The energy drops only when the decaying term is much larger than the growth term. But when the growing term dominates the decaying term, a more common occurrence, a net heating effect occurs. However, there are definitely many points where $|q_{eff,x}|$ exceeds 1, but no significant change in the motional amplitude occurs. The explanation for this curious behaviour is given below.

3.2 The instability time

What is perhaps more important than $q_{eff,u}$ merely exceeding 0.908 is the time interval over which $q_{eff,u}$ has an unstable value. As one can see from Eq. (3.1.3), even in the presence of a distant laser cooled ion, ε_u undergoes a singularity each time the trapping force on the sample ion becomes zero. This occurs at least twice per cycle of the rf-trapping potential. However, when the time period over which $|q_{eff,u}|$ takes an unstable value is short compared to the time interval for the rest of the cycle, the ion amplitute does not significantly grow, hence no measureable heating occurs. Since the ion motion evolves at the secular frequency, a singularity lasting for such a short time interval should not significantly effect the sample ion energy. More significantly, ε_x (or ε_y) also undergoes a singularity as the ion crosses the y (or x) axis. This occurs for each half

cycle of secular motion. The important difference between this and the trapping field singularities is that the instability period can last over a much longer time period as illustrated in Fig. 3.2.1. Here, the solid curve represents the x-component of the trap force on a moving ion as a function of time, and the horizontal dotted lines represent the magnitude of the slowly varying Coulomb force due to another ion. Prior to 0.8 μs, the amplitude of the trap force is large (i.e. the sample ion is not near the y axis) and thus the inter-ionic force dominates only for very short time-intervals as illustrated by A, which is

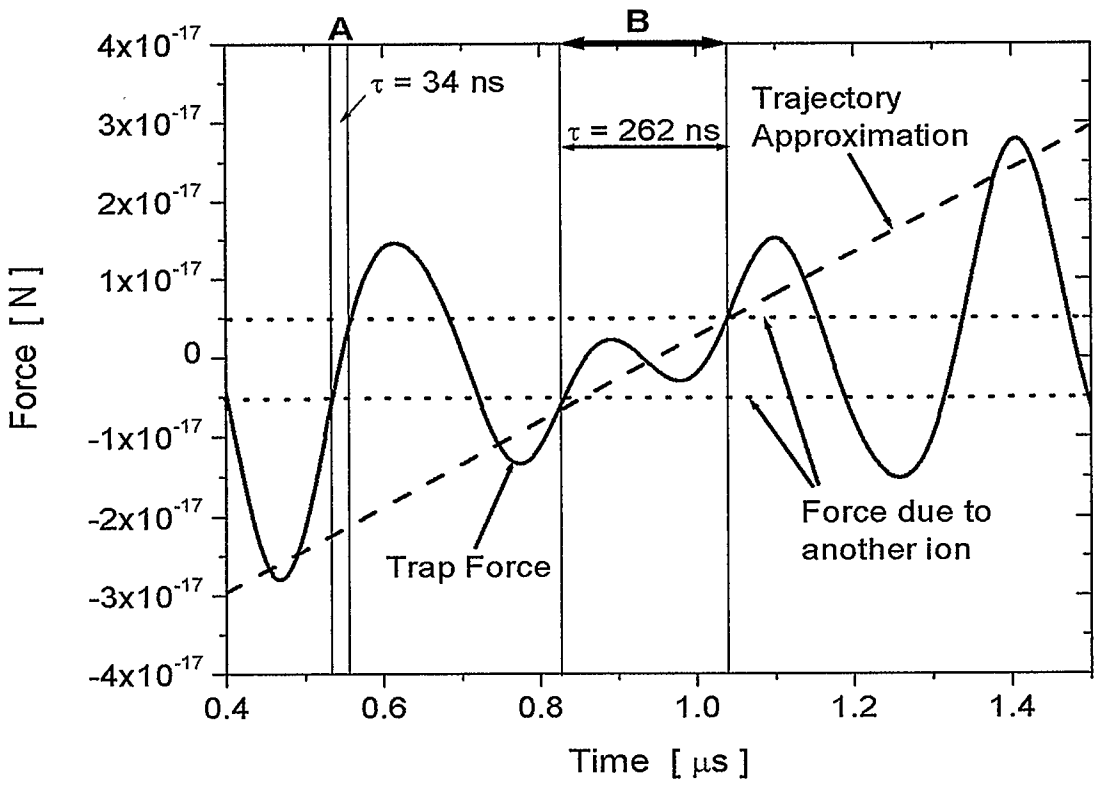

Fig. 3.2.1. A temporal plot of the computed trap force on a moving ion. Point A illustrates the short instability period when the inter-ionic force exceeds the trapping force, while period B illustrates the longer instability period occurring when the secular motion of the ion passes through x = 0.

too short to significantly effect the trajectory of the sample ion. However, when the ion is close to the y axis (i.e. times near 1 μs in this example), the trapping force is weaker than inter-ionic coulomb force if the ion spacing is small enough, as illustrated by event B. This results in measurable heating of the sample ion. The importance of the period over which the ion remains unstable is illustrated by the addition of part (c) of Fig. 3.1.2. We see that the discrete steps in the amplitude of the ion motion occur when $|q_{eff,x}|$ exceeds 1 and does so for a period exceeding 30 to 40 ns. To illustrate this point, three events are highlighted. At point A, $q_{eff,x}$ spikes to well above 1 and the spike lasts for well over 100 ns, resulting in a clear step in the motional amplitude. At point B, there is also an amplitude step, but here $q_{eff,x}$ barely exceeds 1. However, $q_{eff,x}$ stays above the stability threshold for a relatively long time (> 100 ns). On the other hand, at point C there are several spikes all exceeding 1. However, none of the spikes last longer than 20 ns, and the ion motion shows no significant change.

In this chapter we have identified a heating mechanism called instability heating. In the next chapter we will try to predict under what conditions this heating process can prevent sympathetic cooling as the results showed in chapter 2.

4. THE HEATING-COOLING THRESHOLD

4.1 Calculation of the instability heating rate

To generate a predicted shape for the cooling-heating threshold, we need to examine the balance between the heating and cooling rates. To calculate the heating rate, we first need the variation of the mean instability time with the trapping field parameters. From Eqs. (3.1.3) and (3.1.4), the time interval for which $|q_{eff,u}|$ is larger than 0.908 is given by the time interval when

$$|F_{T,u}| \leq \frac{|\langle F_{i,u} \rangle| q_u}{0.908 \pm q_u}. \qquad (4.1.1)$$

is satisfied[7]. The upper sign is used when $F_{T,u}$ and $F_{i,u}$ have opposite sign and the lower sign when they are pointed in the same direction. $\langle F_{i,u} \rangle$ is the average interionic force during a collision. An estimate of this time interval can be obtained as a function of trapping field parameters. The trapping force can be determined by taking the gradient of Eq. (2.1.1) Using Eqs. (2.1.5) and (2.1.6), the force on an ion near the trap centre can be approximated by (see Fig. 3.2.1.)

[7] Remember that we are only interested in trapped ions and thus q must be less than 0.908.

$$F_{T,x}=\frac{ex}{r_o^2}U_{RF}\sin\Omega t'=\frac{eu_o\sin\omega_{sec}t}{r_o^2}U_{rf}\sin\Omega t' \qquad (4.1.2)$$

where t and t′ are used to indicate that the secular and micromotion may be out of phase. Here we have neglected the small effect of micromotion on the x-coordinate of the ion when it is near the trap axis. Given that the time scale of interest is the secular period, much larger than the trapping field period, the trapping field oscillation can be averaged out. Strictly speaking this is zero, but stability is dependent on $|q_{eff,u}| \leq 0.908$. Thus it is really the absolute value of the forces, not their signs which is of interest. Therefore, it is reasonable to replace $\sin\Omega t'$ with its rms value. Also, assuming that we are only interested in times close to the point where the ion crosses the trap axis, the small angle approximation $\omega_{sec}t<<1$ can be used. Thus Eq. (4.1.2) becomes

$$F_{T,x}\approx\frac{eu_o\omega_{sec}t}{2r_o^2}U_{rf}. \qquad (4.1.3)$$

Using Eqs. (2.1.5) and (2.1.6) for ω_{sec} and u_o, we find

$$F_{T,u}=\frac{eU_{rf}}{2r_o^2}\sqrt{\frac{2k_BT}{m_s}}t \qquad (4.1.4)$$

Substituting Eq. (4.1.4). into Eq. (4.1.1), and solving for the instability time τ, we find:

$$\tau \approx \frac{0.908\left|F_{i,u}\right|q_u}{0.908^2 - q_u^2}\frac{r_o^2}{eU_{rf}}\sqrt{\frac{m_s}{2k_BT}}. \qquad (4.1.5)$$

One can see immediately that the instability increases in duration as q_u approaches 0.908, and eventually becomes infinity at the point that q_u reaches the single ion instability threshold.

Given Eq. (4.1.5.), we can calculate the heating rate by also considering the collision rate, the frequency at which these axis-crossings happen, and the rate at which the energy grows during the instability. The collision rate is simply a function of the number of trapped ions and the trapping volume, while the axis crossings occur at twice the secular frequency[8]. To determine the rate of energy growth during the instability, we must calculate how rapidly the radius of the ion trajectory grows. The parameter μ in Eq. (2.1.4.) governs this growth. Since $q_u = 0.908$ marks the transition from imaginary to complex values for μ, this coefficient, at least near the transition point, should take the form

$$\mu = \eta\sqrt{|q_u| - 0.908}, \qquad (4.1.6)$$

[8] This is true even in the presence of other ions, since the ionic gas is so diffuse.

where η is a constant of order unity. This cannot be shown analytically for the Paul trap. However, for the closely related rotating saddle trap that can be solved analytically, μ takes the form of Eq. (4.1.6). with η=1 [27]. Converting back from unitless parameters, the rate of exponential growth in the motion during the instability is given by:

$$\mu\Omega/2 = \tfrac{1}{2}\eta\Omega\sqrt{\left|q_{\mathrm{eff},u}\right| - 0.908}\,, \tag{4.1.7}$$

while the rate of energy increase is simply twice this amount due to the harmonic nature of the potential. Here, q_u has been replaced with $q_{eff,u}$ since it is this quantity that reaches unstable values, not q_u. We will approximate Eq. (4.1.7.) using a mean value for $q_{eff,u}$ by assuming $F_{i,u}$ to be roughly constant over the instability period and that $F_{T,u}$ can be replaced by the average of its maximum magnitude during instability and its minimum value of zero (see Eq. (4.1.1.)). When $q_{eff,u}$ for parallel and anti-parallel forces are averaged, the result is independent of q_u, leaving an average value for the exponential growth rate of

$$\langle\mu\Omega/2\rangle = \tfrac{1}{2}\eta\Omega\sqrt{0.908}\,. \tag{4.1.8}$$

Finally, taking the heating rate to be proportional to the instability time, the energy growth rate, the collision rate (σ_{coll}), and the axis crossing frequency ($2\omega_{sec}$) yields

$$R_h = \frac{0.908|F_{i,u}|q_u}{0.908^2 - q_u^2}\frac{\eta\sigma_{coll}}{4\pi}\sqrt{\frac{0.908}{m_s k_b T}}. \qquad (4.1.9)$$

4.2 The cooling Rate

To avoid overall heating of the ions, R_h must be balanced by the cooling effect, which occurs via elastic collisions between slow and fast moving particles of different masses. Simple classical mechanics arguments show that the efficiency of elastic collision energy transfer decreases as the mass difference between the particles increases. The energy transfer efficiency is given by $4\rho/(1+\rho)^2$, where $\rho = m_s/m_c$ [14]. Taking the cooling rate to be proportional to the product of this efficiency and the collision rate gives

$$R_c = K_c\sigma_{coll}\frac{m_s/m_c}{(1+m_s/m_c)^2}. \qquad (4.2.1)$$

It is also important to note that the cooling process, being statistical in nature, depends on both the temperatures of the laser cooled ions, and sample ions. This temperature dependence has been absorbed into K_c for now, but will be discussed later on, in Chapter

5. When the two rates balance, we should see a transition from heating to cooling of the sample ions. Equating Eqs. (4.1.9) and (4.2.1.), we obtain

$$\frac{q_u}{0.908^2 - q_u^2} = \frac{4\pi K_c}{0.908|F_{i,u}|\eta}\sqrt{\frac{k_b T}{0.908}}\frac{\sqrt{m_s^3}/m_c}{(1+m_s/m_c)^2}. \qquad (4.2.2)$$

The collision rates in Eqs (4.1.9) and (4.2.1) have been taken to be the same. This is valid if the number of laser-cooled ions significantly exceeds the number of sample ions. In general, cooling occurs when sample ions collide with the laser-cooled ions, while instability heating is caused by interactions between any two ions. However, if most of the ions in the trap are laser-cooled ions, then most of the instability heating is a result of interactions between sample ions and laser cooled ions. This means that both the heating and cooling rates are proportional to the same collision rate, and so this rate cancels out. Therefore, the rate of collisions determines the rate of heating or cooling and not the sign of the temperature change.

4.3 The effect of mass on the heating cooling threshold

Equation (4.2.2) provides the theoretical justification that lines of constant q_u define the heating-cooling boundaries in U_{rf}-Ω space. Although we cannot calculate threshold values for q_u from first principles, because of the unknown scaling factors, it can be done

numerically. This was done to produce the $q_u = 0.509$ curve in Fig. 2.3.4, showing that this line effectively separates the regions of heating and cooling. Once the threshold value of q_u is determined for one mass combination, Eq. (4.2.2) can be used to determine the value for other mass combinations. This is illustrated by the $q_u = 0.408$ line in Fig. 2.3.3. This line was not fit to the data, but rather it was calculated from the constant value for Fig. 2.3.4. It should be noted that this model has been applied only to a limited mass range and that perhaps other mass effects have to be included if very large mass changes are required.

Up to this point, we have concentrated mainly on the effect of the mass of the sample ion. However, the laser-cooled ion mass is also significant. This is because the efficiency of energy transfer between two colliding particles decreases as the ratio of the masses deviates from unity, becoming effectively zero when one mass is negligible as compared to the other. However, the instability-heating rate is expected to be relatively unchanged as it results from the Coulomb interactions between the ions and with the trapping field. Thus for larger mass ratios, the heating-cooling threshold should move further from the single-ion instability threshold in order to reduce the level of instability heating that must be overcome. This reduces the overall collision rate, which decreases the rate of heating or cooling of the sample ion. The effect of laser-cooled ion mass was examined by running simulations with 18 amu sample ions interacting with either 24 amu or 36 amu laser cooled ions for a range of q_u. The results are summarized in Table 4.2.1. which illustrates the expected slight shift in the cooling-heating threshold for different laser-cooled ion masses.

q_u	$\Omega/2\pi$ [MHz]	U_{rf} [V]	m_c=24 amu	m_c=36 amu
0.19	2	70	**C**	**C**
0.25	2.5	40	**C**	**C**
0.35	1.5	20	**C**	**C**
0.38	2.5	60	**C**	**C**
0.39	2	40	**C**	**C**
0.43	2.54	70	**C**	**C**
0.47	2.43	70	**C**	N
0.51	2.5	80	N	N
0.59	2	60	N	N
0.61	3	140	N	**H**
0.63	2.5	100	N	**H**
0.66	2.05	70	N	**H**
0.70	1.5	40	**H**	**H**
0.76	2.5	120	**H**	**H**

Table. 4.2.1. Computational observations of sympathetic heating or cooling for different trapping field parameters for 5 sample ions (mass 18 amu) interacting with 35 laser cooled ions (either mass 24 amu or mass 36 amu). The sample ion behavior was categorized, based on a 60 ms evolution, into heating (**H**), cooling (**C**), or no observed temperature change (N).

These results are in good agreement with the heating-cooling transition values predicted by Eq. (4.2.2) based on the 12 amu-24 amu threshold. The predicted heating-cooling threshold values are 0.585 for 18 amu-24 amu and 0.56 for 18 amu-36 amu.

Chapters 2 through 4 have provided some insight into the conditions under which sample ions heat or cool due to sympathetic laser cooling. However, it would be very useful to determine the limiting temperature that the ions will reach under heating or cooling conditions. Chapter 5 will attempt to address this question.

5. THE EQUILIBRIUM TEMPERATURE

5.1 Introduction

As we have seen, ions in the gaseous phase are prone to instability heating, the degree of which has been determined to be a function of q,[9] the instability parameter. To cool a sample of ions sympathetically, the cooling rate, which results from collisions between the refrigerant laser-cooled ions and the hot sample ions, must be larger than the instability heating rate, so that overall sample ion cooling is achieved. However, since the cooling portion of the overall energy transfer process is purely statistical, the ions one wishes to sympathetically cool must be hotter than the laser cooled ions for a finite cooling rate to exist in the first place. It is seen in our simulations that an equilibrium temperature is reached when the temperature difference between the sample ions and laser cooled ions results in a sufficiently large cooling rate to be able to balance the instability heating rate. A relationship between q and the equilibrium temperature is seen, suggesting that as q approaches zero, the sample ion temperature T_S approaches that of the laser cooled ion temperature T_l. This requirement that $T_s > T_l$ at finite q means that the equilibrium temperature of the sympathetically cooled sample ions is always hotter than that of the laser-cooled ions due to the presence of instability heating, which, not being a statistical process, is ever present upon collisions and prevents the sample ions from reaching thermal equilibrium with the laser cooled ions.

---

[9] For a symmetric trapping potential q_x and q_y are identical and therefore we will use q instead of q_u.

5.2 Numerical simulation results

The basic computational set up is identical to that described earlier, except that we have used 15 sample ions instead of 5 and 45 laser cooled ions instead of 35. The increase in the number of ions was necessary in order to smooth the output data upon averaging over the sample and laser cooled ion energies, the output data being plots of sample ion temperature vs time. The sample ions were started at 50 K, and were allowed to interact with the 15 K laser-cooled ions. Both species were also subject to the trapping forces described earlier. The numerical integration was carried out over 60 ms. This was observed to be a sufficient length of time to allow the sample ions to reach an equilibrium situation. The laser-cooled ions were fixed at 15 K by computationally laser-cooling them (see page in reference [22]) whenever each of the temperatures associated with their different degrees of freedom rose above 15 K.

For these experiments, we used sample ion masses of 12 amu and 8 amu, and a laser-cooled ion mass of 24 amu. It is expected that any results using these particular masses will easily generalize to other mass combinations. The physical significance of varying the mass was discussed earlier. In our computational experiment we varied q, the stability parameter, by varying the trapping parameters U_{rf} and Ω only; this can be done more easily in the lab than by varying the mass. From our theory of instability heating , it has been found that ions of mass 12 amu, interacting with ions of 24 amu, will only cool if $q < 0.50$ and will heat if $q > 0.50$. However, as we shall see, 'cool' and 'heat' here, mean only with respect to their initial temperature of 50 K. Figure. 5.2.1 shows three

plots of sample ions of q = 0.40, 0.57, 0.26. In Fig. 5.2.1(a), starting at 50 K, the sample ions cool, since q < 0.50, but only down to 28 K, then stop cooling. In Fig. 5.2.1(b), the sample ions heat, since q > 0.50, but only up to 80 K, then stop heating. In Fig. 5.2.1(c) the sample ions cool down to 17 K, then stop cooling. Our data suggests that q, rather than being an overall parameter that determines whether or not a sample will cool or heat

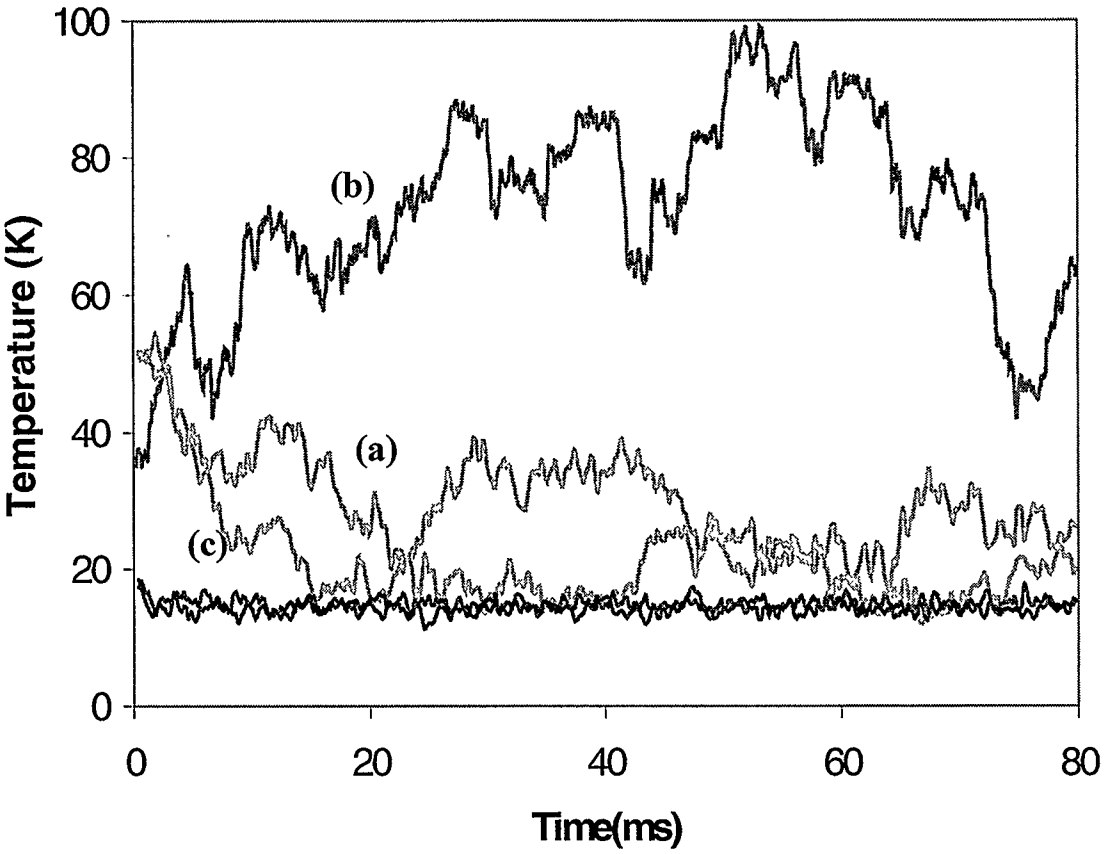

Fig. 5.2.1. Temperature of sympathetically cooled ions vs Time. In each plot the sample ion mass is 12 amu and the Laser- cooled ion mass is 24 amu. The laser cooled ions are kept at 15 K. The values of q where changed by varying the trapping parameters U_{rf} and Ω. Line (a) is for q = 0.4 and yields a final temperature of 28 K, line (b) is for q = 0.57 and yields a final temperature of 80 K, line (c) is for q = 0.26 and yields a final temperature of 17 K

regardless of initial temperature, is in fact a measure of the final temperature of the sample ions and therefore acts as a thermodynamic state variable. Consider for example the last case, for which q = 0.26, and the ions cooled from 50 K down to 17 K. Suppose now we had started the sample ions at 17 K, in this case the ions would neither have cooled nor heated, and this value of q would have marked a heating-cooling boundary.

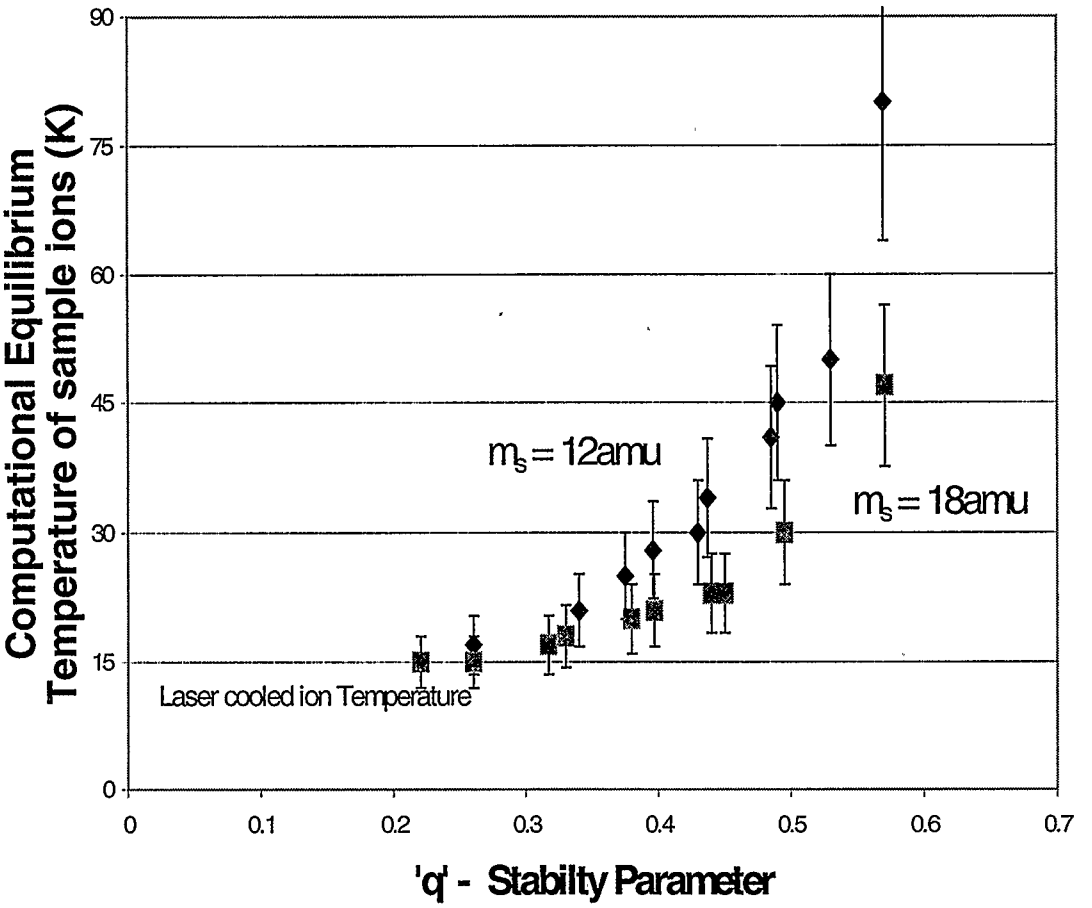

Fig. 5.2.2. Computational results of Equilibrium Temperature vs 'q' of sympathetically cooled sample ions. The sample ion mass is 12 amu (diamonds) and 18 amu (squares). The Laser- cooled ion mass is 24 amu. The laser-cooled ions are kept at 15 K.

So clearly q = 0.50 for m_s = 12 amu, is not a boundary in the absolute sense, but merely correspond to the equilibrium temperature of 50 K. Likewise q = 0.26 for m_s = 12 amu, corresponds to the equilibrium temperature of 17 K. Figure. 5.2.2, shows all of our data points of q vs the equilibrium temperature of the sample ions T_{se}. From this, we see that as q increases, so does the equilibrium temperature of the sample ions away from T_l.

5.3 The Equilibrium Temperature theory

In this section, we examine the heating rate and cooling rate independently, then equate them to determine an equation for the equilibrium temperature. We will develop an expression for the cooling rate first, that takes into account the temperatures of the two species. Eq. (4.2.1) gives the cooling rate expression as

$$R_c = K_c \sigma_{coll} \frac{m_s/m_c}{(1+m_s/m_c)^2} \qquad (5.3.1)$$

which was taken at a particular temperature difference. That is to say, the equilibrium temperature difference, that led to an overall sympathetic cooling rate of zero, by equating it to the heating rate. This defined lines of constant 'q' as heating - cooling boundaries, which depend on the mass of the sample ion. Taking the temperature of the sample ion into account instead of the mass in the expression for R_c, will allow us to take one step further, and instead of asserting that lines of constant 'q' just mark absolute

heating-cooling boundaries, it will allow us to say, to what temperature the sample will heat or cool either side of this boundary.

For this calculation we will absorb the term involving the mass ratio of the sample ions and laser cooled ions into a constant, and re-extract it at the end just to save writing it out at each step. Assuming that throughout the cooling process we can characterize the laser cooled ions (reservoir) and sample ions by temperatures T_l and T_s, respectively, the rate at which the sample ions cool is simply related to the probability that the combined system will choose a state in which T_s is lower, and the rate at which it chooses, i.e. the collision rate. Qualitatively, we expect, that as T_s approaches T_l, since the number of states function for the system approaches a maximum, the probability of choosing a state in which T_s is lower, approaches a half, and the cooling rate goes to zero.

This can be made quantitative using the following statistical mechanics argument. First we will assume that the collision rate is constant, and that the combined system goes from state to state at a constant rate. In this case, the variation of the cooling rate of the sample ions is brought about by the variation of the number of states function alone (see Fig. 5.3.1)

The number of states accessible to the combined system, when the sample ions have energy E_s, is $\Omega(E_s)$. After a unit of time, the sample ions now have energy $E_s - \Delta E_s$, given by

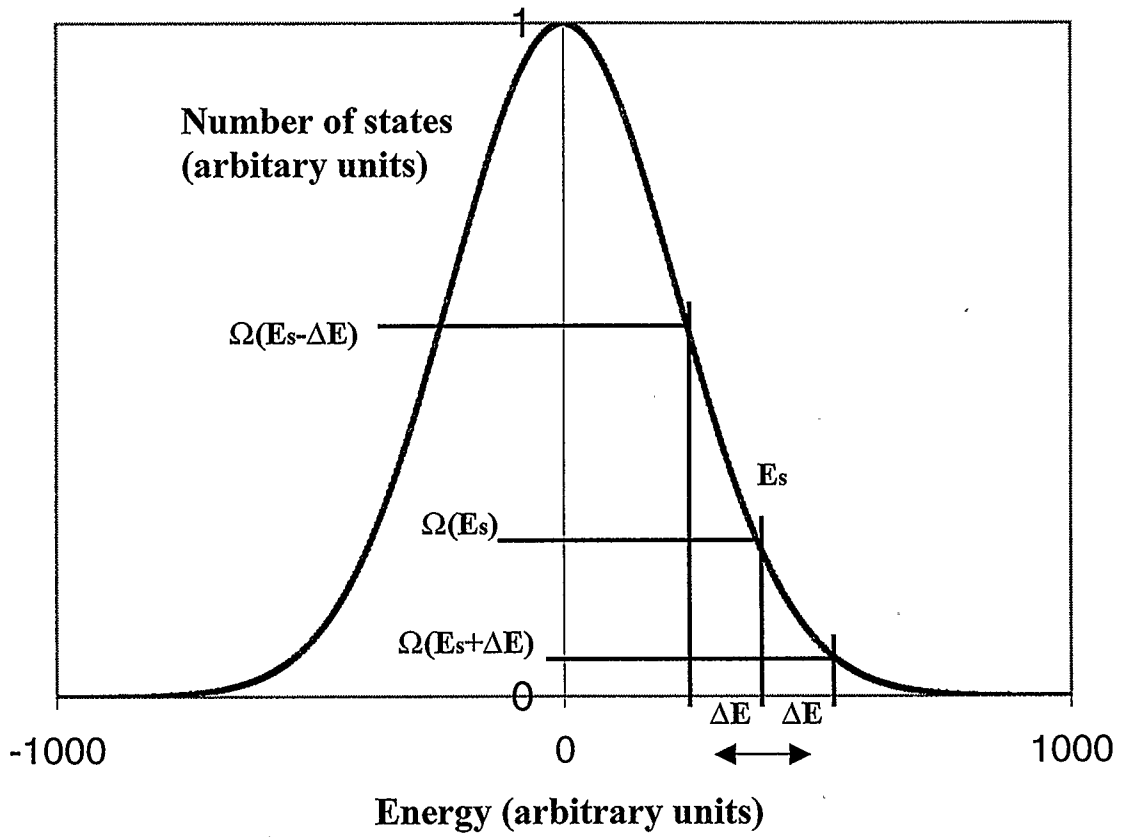

Fig 5.3.1. Total number of states function vs Energy of sample ions. At each time unit each ensemble either increases or decreases it's energy by ΔE through exchange with the laser cooled ions. Sample ion cooling is brought about due to the fact that more systems in the ensemble decrease their energy than increase it, as shown above.

$$E_s - \Delta E_s = \frac{(E_s - \Delta E)\Omega(E_s - \Delta E) + (E_s + \Delta E)\Omega(E_s + \Delta E)}{2\Omega(E_s)} \qquad (5.3.2)$$

where ΔE is a finite amount of energy either gained or lost by each system in our ensemble, in our allotted unit of time, Δt.

and since ΔE is small we can say that

$$\Omega(E_s) = \frac{\Omega(E_s - \Delta E) + \Omega(E_s + \Delta E)}{2} \tag{5.3.3}$$

Multiplying out the brackets in Eq. (5.3.2.) the energy can be expressed as

$$E_s - \Delta E_s = \frac{E_s[\Omega(E_s - \Delta E) + \Omega(E_s + \Delta E)] - \Delta E[\Omega(E_s - \Delta E) + \Omega(E_s + \Delta E)]}{2\Omega(E_s)} \tag{5.3.4}$$

Using Eqs. (5.3.3.) and (5.3.4.) and canceling the E_s gives

$$\Delta E_s = \frac{1}{2}\frac{\Omega(E_s + \Delta E) - \Omega(E_s - \Delta E)}{\Omega(E_s)}\Delta E \tag{5.3.5}$$

Since ΔE is just a finite constant, we can multiply Eq. (5.3.5.) by $\Delta E / \Delta E$,

$$\Delta E_s = K \frac{\Omega(E_s+\Delta E) - \Omega(E_s-\Delta E)}{\Omega(E_s)\Delta E} \Delta E^2 \qquad (5.3.6)$$

When ΔE is sufficiently small, but not zero, we can approximate Eq. (5.3.6) by

$$\Delta E_s = K \Delta E^2 \frac{\partial \ln \Omega(E_s)}{\partial E_s} \qquad (5.3.7)$$

and since the above equation is per collision, we can generate the rate of energy change by multiplying Eq. (5.3.7) by the collision rate σ_{coll} to yield

$$\frac{dE_s}{dt} \approx \Delta E_s \sigma_{coll} = K' \frac{\partial \ln \Omega(E_s)}{\partial E_s} \sigma_{coll} \qquad (5.3.8)$$

where the ΔE^2 has been absorbed into the new constant. We can now incorporate the rate at which states are chosen, by multiplying this by the collision rate to give the overall cooling rate R_c.

$$R_c = -\frac{dE_s}{dt} = -K' \frac{\partial \ln \Omega(E_s)}{\partial E_s} \sigma_{coll} \qquad (5.3.9)$$

This can be expressed in terms of the temperatures of the sample ions, and the laser cooled ions. Since $\Omega(E_s)$ is the total number of states function, we can express it as a

product of the number of states function for the sample ions and the number of states function of the laser cooled ions[10].

$$\Omega(E_s) = \Omega_l(E_l)\Omega_s(E_s) \tag{5.3.10}$$

Eq. 5.2.1 can now be expressed as,

$$R_c = -\frac{dE_s}{dt} = -K\frac{\partial \ln\Omega_l(E_{total}-E_s)\Omega_s(E_s)}{\partial E_s}\sigma_{coll} \tag{5.3.11}$$

This can be expanded as follows

$$R_c = K'\left(\frac{\partial \ln\Omega_l(E_l)}{\partial E_l} - \frac{\partial \ln\Omega_s(E_s)}{\partial E_s}\right)\sigma_{coll} \tag{5.3.12}$$

The minus sign merely reflects the fact that the change in energy of the sample ions, is opposite in sign to the change in energy of the laser cooled ions. In this form, we can use the definition of temperature in terms of the density of states to express cooling rate in terms of the temperatures of the laser cooled ions and sample ions.

[10] The following few steps (5.3.10) - (5.3.13) can be justified and found in any statistical mechanics text. i.e. [28]

$$R_c = K'\left(\frac{1}{k_b T_l} - \frac{1}{k_b T_s}\right)\sigma_{coll} \qquad (5.3.13)$$

Here k_b is Bolzmanns constant. This can be expressed as,

$$R_c = \frac{K'}{T_l}\left(1 - \frac{T_l}{T_s}\right)\sigma_{coll} \qquad (5.3.14)$$

Since the cooling rate is also related to the mass ratio (see Eq. (5.3.1.)), we will extract this from the constant appearing in Eq. (5.2.4.)

$$R_c = \frac{K''}{T_l}\left(1 - \frac{T_l}{T_s}\right)\frac{m_s/m_c}{(1+m_s/m_c)^2}\sigma_{coll} \qquad (5.3.15)$$

The heating rate as given in section 4.1 is given here, only we have absorbed all of the constants into K_h and explicitly included the collision rate.

$$R_h = \frac{K_h q_u \sigma_{coll}}{0.908^2 - q_u^2}\frac{1}{\sqrt{m_s T_s}} \qquad (5.3.16)$$

Now that we have extracted all of the temperature dependence from the heating and cooling rates we can equate them to find the equilibrium temperature.

$$\frac{K_f}{T_l}\left[1-\frac{T_l}{T_{se}}\right]\frac{m_s/m_l}{(1+m_s/m_l)^2}=\frac{q_u}{0.908^2-q_u^2}\frac{1}{\sqrt{m_s T_{se}}} \qquad (5.3.17)$$

Here, K_f is just a constant, taking into account all the constants appearing in Eqs. (5.3.15) and (5.3.16). By choosing a suitable value for K_f, we can fit Eq. (5.3.17) to the data in Fig 5.2.2 for one of the masses, say $m_s = 12$, then using this value of K_f we can fit Eq. (5.3.17) to the data for $m_s = 18$ in Fig 5.2.2. Although Eq. (5.3.17) does not fit exactly, it does exhibit all of the important properties we would have expected. At q = 0, the

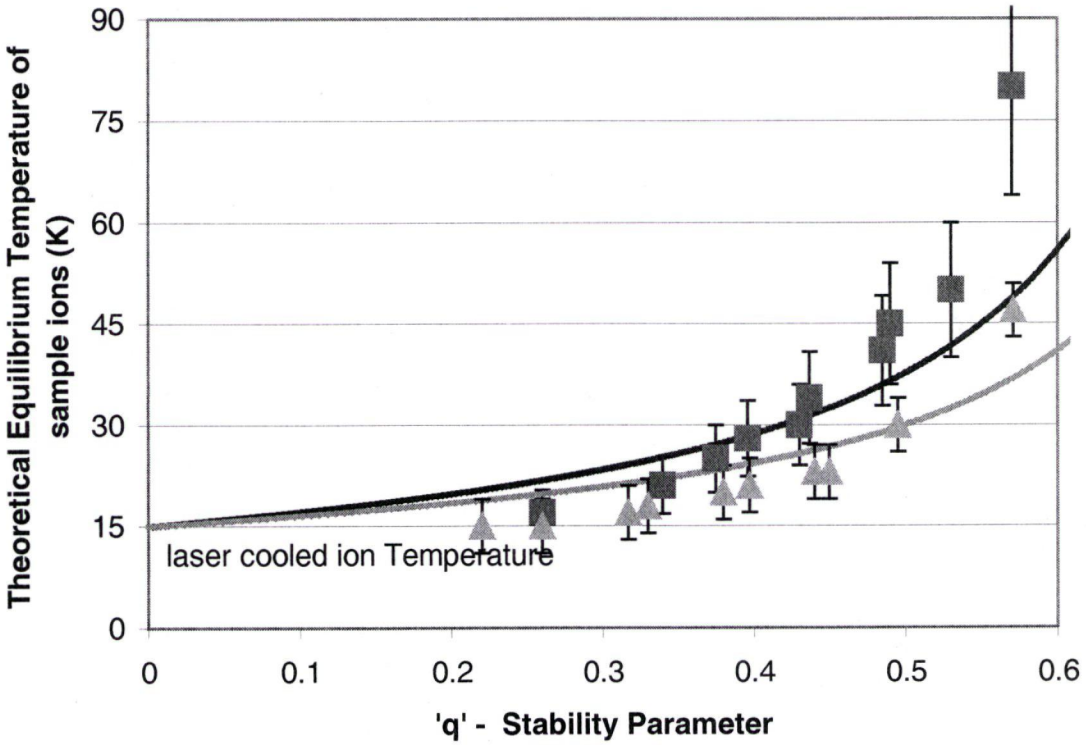

Fig. 5.3.2. A plot of equilibrium temperature vs Stability Parameter 'q' for $m_s = 12$ (squares) and $m_s = 18$ (triangles). The solid lines are Eq. 5.2.3. fit to th e12 amu data, and then calculated for the 18 amu curve.

equilibrium temperature goes to T_l, since the heating rate goes to zero, and as q approaches 0.908 the equilibrium temperature approaches infinity, since the heating rate approaches infinity. The theoretical fit does however seem to be systematically off, in that our predicted value of T_{eq} does not increase fast enough with respect to q. Upon adjusting Eq. (5.3.17) to see what would make it a better fit, it was found that an extra factor of q on the heating side of the equation would yield a much better result. The justification for this proved somewhat more difficult. Our best guess as to the missing factor of q may lie in our rather crude step of canceling the collision rates[7]. Firstly, we ignored collisions between the sample ions themselves. This would cause additional heating since these collisions have no cooling capability. Secondly, we ignored the possibility that the collision cross sections for cooling type collisions and heating type collisions may be different. Both of these reasons would have prevented a cancellation of the collision rates.

On the other hand, the problem could be that our theoretical fit is fine but that our computational data is systematically off. It could be the case that as q increases, more error builds up during the integration. This would make sense, since large values of q are linked to rapid periods of growth (see Eqs. (4.1.6) and (2.1.4)), and these are integrated much less accurately than less rapid motion, causing energy to slowly build up in the system.

---

[7] This was done since the mechanism that causes both heating and cooling, results from collisions between laser cooled ions and sample ions only (see end of section 4.2).

Ignoring the slight systematic offset, we see that for a given temperature of laser cooled ions, which in our computational experiments was set at 15 K, the equilibrium temperature T_{se} of the sample ions only depends on q, the stability parameter of the ion trap, indeed rendering q a state variable, which is what our computational data suggested.

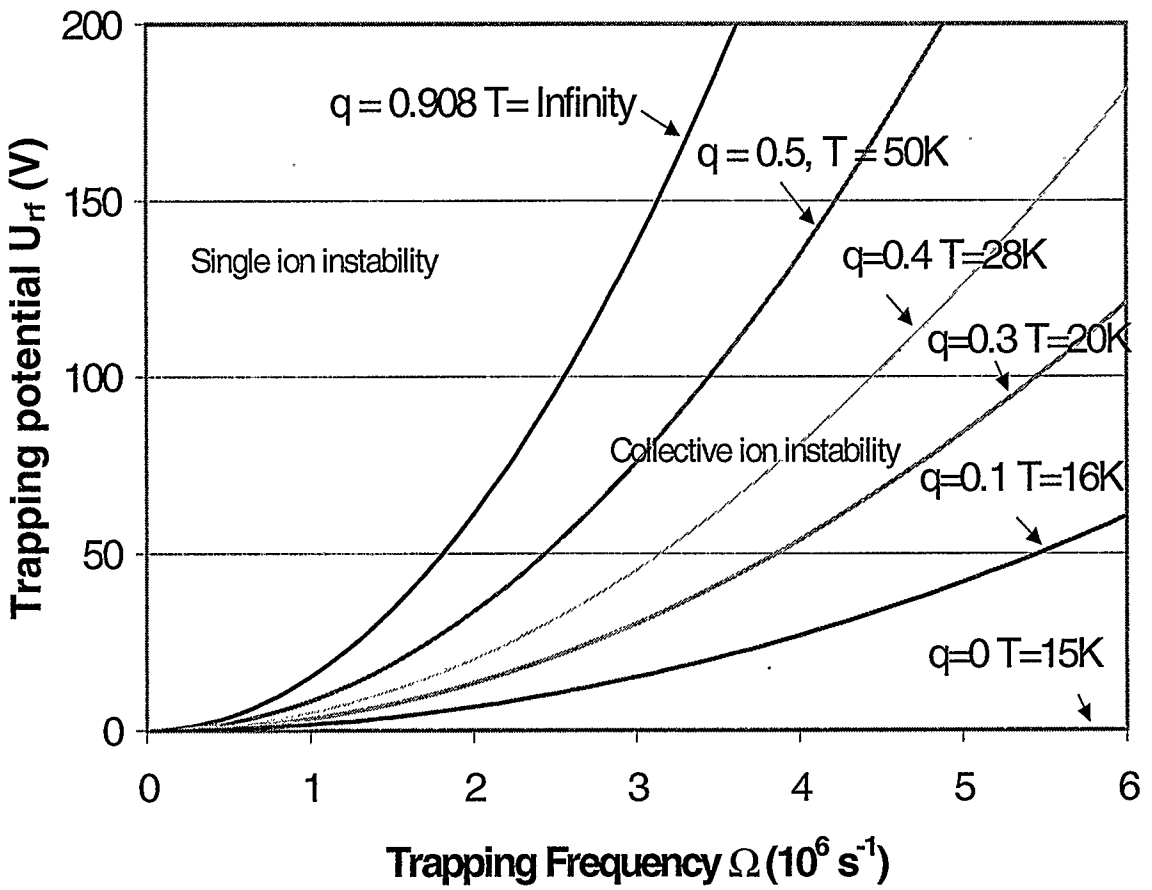

Fig. 5.3.3. Lines of constant q and T, in U_{rf}-Ω space, for sample ions of mass 12 amu and laser cooled ions of mass 24 amu kept at 15 K.

Since there exists a relationship between q and T_{se}, we can associate lines of constant 'q' in the U_{rf} and Ω (Trapping parameters) space, with lines of constant T_{se}, and thus relate the trapping parameters, which are easily controllable in the lab to a measurable quantity, that being the temperature of the ions. Figure. 5.3.3 shows a plot of lines of constant q and T_{se}, in U_{rf} - Ω space. As before, what this shows, is that by reducing q to a new lower value, we can cool the sample ions below the temperature associated with their initial value of q, but here we see that the sample ions cool only as far as the temperature associated with this new value of q.

6. DISCUSSION AND FUTURE DIRECTIONS

The results of the preceding sections provide us with a physical insight into the competing processes that lead to sympathetic heating or cooling of ion mixtures. Generally speaking, we can conclude that if sympathetic heating is occurring for light sample ions, the trap parameters can be adjusted to move away from the single ion instability threshold, thereby allowing the sample ions to cool. However, there is a limit to this effect. As one moves far away from the instability threshold, as would be needed to cool very light ions, the trapping field becomes weaker, the trapping volume grows, and the collision rate becomes very small. Although an ion still cools, the rate of cooling may be so small as to be of little practical use.

Instability heating is to be distinguished from rf heating [17,29]. This transient effect is caused by random interactions between ions, temporarily driving them into unstable motion. In contrast, rf heating of the ions near the quadrupole axis is caused by continous coulomb interactions with the ions which are constantly driven by the rf field at the periphery. Rf heating cannot be suppressed solely by changing the trap parameters, only by reducing the number of ions and cooling the sample to the point where all of the ions crystallize along the central axis of the trap where micromotion is not present. However, instability heating, which is a major source of heating in the low-density gas phase regime, can be quenched by choosing favorable trap parameters so that the ions are less susceptible to heating. This is achieved by minimizing the duration of potentially

unstable motion and the frequency at which these potential instabilities occur, so that in the event of a collision an ion is more likely to decrease its energy.

Further theoretical work is needed to study the effect of changing the relative numbers of sample and laser cooled ions. When the number of sample ions increases, the interactions between them can no longer be ignored. This will ultimately cause more heating, since such interactions cannot result in a decrease in the mean energy. Although Eq. (4.1.9) suggests that instability heating should decrease in the higher energy regime this has yet to be tested; such collisions at high temperatures (~300 K) require much more computational time and other techniques may need to be developed to model them. At low energies (~1K) Eq. (4.1.9), which is applicable for ions in the gas phase, becomes less valid since the ions are in the crystalline phase. Instability heating is expected to be insignificant here since the axial separation is always large enough to prevent the transverse forces, which cause instabilities, from becoming too large. The dominant heating mechanism in this low energy crystalline phase would be rf-heating when the ion number is large. Of course, since none of this has been demonstrated in the lab, experimental work is needed to empirically verify the results presented in this work.

In this work, we have ignored the internal degrees of freedom of the sample ions, which is reasonable if the ions are all atomic, but less so in the case of molecular sample ions. The distinction between sample atomic ions and sample molecular ions was deliberately overlooked, since the focus of this work is the translational degrees of freedom. In ignoring the molecular ions' internal structure we have a first order approximation as to whether or not the sample molecular ions will translationally heat or

cool. Translational cooling in this approximation is seen as a significant component of a complete model of the sympathetic cooling. This is because another major energy transfer process is expected to be intramolecular transfer of energy from rotational and vibrational modes to translational degrees of freedom followed by interionic translational energy transfer to the laser-cooled atoms, as modeled in this work.

7. CONCLUSION

The mechanism through which sample ions are heated in a linear Paul trap is a direct result of collisions, the same collision that would otherwise bring about thermal equilibrium at a lower temperature. A collision can cause an ion to become briefly unstable and thus rather than energy being transferred to the laser cooled ion for dissipation in the radiation field, kinetic energy is pumped into the ion from the electric fields if its $q_{eff,u}$ is greater than 0.908. This heating mechanism is to be distinguished from rf-heating [14,20] which refers to the heating of ions near the quadrupole axis by Coulomb interactions with those at the periphery which are constantly driven by the rf field. Rf-heating cannot be suppressed solely by changing the trap parameters, only by reducing ion numbers and cooling the sample to the point where all the ions crystallize along the central axis of the trap where micromotion does not exist. However, instability heating, which is a major source of heating in the low-density gas phase regime, can be quenched by choosing favourable trap parameters so that the ions are less vulnerable to heating. This is achieved by minimising the duration of potentially unstable motion and the frequency at which these potential instabilities occur, so that in the event of a collision the ion is more likely to decrease its energy. We have shown that this occurs when q_u is small. Since q_u is a function of mass, trap frequency and trap depth a lower mass limit will exist below which sample ions will heat, only for fixed trapping parameters (Eq. (13.)). This mass limit corresponds to a second characteristic threshold

value for q_u, above which heating will occur [15]. More generally, there exists a region of mass, trap frequency and voltage space corresponds to a region of high instability and thus heating, constraining any two of these variables will result in an upper or lower limit in the third.

The final equilibrium temperature of gaseous sample ions interacting with gaseous laser cooled ions in a Linear Paul Trap is a result of a competition between a statistical cooling rate, and a instability heating rate. Since the cooling portion of energy transfer process is purely statistical, the cooling rate drops to zero as T_s approaches T_l. However, the heating rate, which is not a statistical process, but caused by collisional instabilities, then dictates that the sample ions can never come into thermal equilibrium with the laser-cooled ions. We have shown that by controlling q, through the trapping parameters U_{rf} and Ω, we can control the equilibrium temperature of the sample ions. Also, by sufficiently reducing 'q', and hence the heating rate, one can bring the ions into effective thermal equilibrium with the laser cooled ions.

BIBLIOGRAPHY

[1] See for example the many excellent papers in *Coherent and collective interactions of particles and radiation beams*, Proc. International School of Physics "Enrico Fermi", Course CXXXI, A. Aspect, W. Barletta and R. Bonifacio (Eds.), (IOC Press, Amsterdam, ,1996); *Frontiers in laser spectroscopy*, Proc. International School of Physics "Enrico Fermi", Course CXX, T.W. Hänsch and M. Inguscio (Eds.), (North-Holland, Amsterdam, 1994); *Laser Manipulation of Atoms and Ions*, Proc. International School of Physics "Enrico Fermi", Course CXVIII, E. Arimondo, W.D. Phillips, F. Stumia (Eds.), (North-Holland, Amsterdam, 1992).

[2] M. Kasevich and S. Chu,: Appl. Phys. B **54**, 321 (1992).

[3] C. J. Pethick and H. Smith : *Bose-Einstein Condensation in Diliute Gases,* (Cambridge University Press, 2002), p.264.

[4] I.b.i.d. P. 16.

[5] I.b.i.d. P. 7.

[6] S. Chu, L. Hollberg, J.E. Bjorkland, A. Cablea, and A. Ashkin: Phys. Rev. Lett. **55**, 48 (1985).

[7] P. Lett, R. Watts, C. Westbrook, W. Phillips, P. Gould, and H. Metcalf: Phys. Rev. Lett. **61**, 169 (1988); J. Dalibert, C. Cohen-Tannoudji: J. Opt. Soc. Am. B **6**, 2023 (1989); M. Kasevich, S. Chu: Phys. Rev. Lett. **69**, 1741 (1992).

[8] B. Sheehy, S-Q. Shang, R. Watts, S. Hatamian, and H. Metcalf: J. Opt. Soc. Am. B **11**, 2165 (1989).

[9] J.T. Bahns, W.C. Stwalley, and P.L. Gould: J. Chem. Phys. **104**, 9689 (1996).

[10] D.J. Larson, J.C. Bergquist, J.J. Bollinger, W.M. Itano, and D.J. Wineland: Phys. Rev. Lett. **57**, 70 (1986).

[11] A.C. Truscott; K.E. Strecker; W.I. McAlexander, G.B. Partridge, and R.G. Hulet: Science **291**, 2570 (2001).

[12] K. Molhave and M. Drewsen: Phys. Rev. A **62**, 011401 (2000).

[13] P. Bowe and L. Hornekaer : Phys. Rev. Lett. **82**, 2071 (1999).

[14] T. Baba and I. Waki, Jpn. J. Appl. Phys. **35**, L1134 (1996).

[15] T. Baba and I. Waki : J. Appl. Phys. B **74**, 375 (2002).

[16] D. J. Wineland and J. C. Berguist : Phys. Rev. Lett. **59**, 2935 (1987).

[17] W. Paul, E. Arimondo, W.D. Phillips, and F. Stumia (Eds.), *Laser Manipulation of Atoms and Ions*, Proc. International School of Physics "Enrico Fermi", Course CXVIII, (North-Holland, Amsterdam,1992), 492.

[18] T. J. Harmon, N. Moazzan-Ahmadi, and R. I. Thompson: Phys. Rev. A **67**, 013415 (2003).

[19] R.E. March and R.J. Hughes, *Quadrupole Storage Mass Spectrometry*, (Wiley and Sons, New York, 1989).

[20] P. Dawson, *Quadrupole Mass Spectrometry and its applications*, (Elsevier, Amsterdam, 1976).

[21] F. M. Arscott, *Periodic Differential Equations* (Pergamon Press, Oxford, 1964)

[22] H. J. Metcalf and P. Van der Staten, *Laser Cooling and Trapping*, (Springer,New York,1999), p.88.

[23] D.J. Wineland, J.C. Bergquist, W.M. Itano, J.J. Bollinger , and C. H. Manney: Phys. Rev. Lett, **59**, 2936 (1987).

[24] G. Birkl, S, Kassner & H. Walther: Nature, **357**, 310 (1992),

[25] P. Bowe, L. Hornekaer, C. Brodersen, M. Drewsen, and J.S. Hangst: Phys. Rev. Lett, **82**, 2071 (1999).

[26] M. Welling, H. A. Schuessler, R. I. Thompson, and H. Walther: International Journal of Mass Spectrometry and Ion Processes **172,** 95 (1998).

[27] R.I. Thompson, T.J. Harmon and M. Ball: Can. J. Phys. **80**, 1433 (2002).

[28] F. Reif : *Fundamentals of statistical mechanics*, (McGraw Hill, 1965), P. 96.

[29] M. Drewsen, and A. Broner: Phys. Rev. A **62**, 045401 (2000).

Appendix A

The Euler Picard Predictor-Corrector Method

Our computer simulation numerically integrates the classical equation of motion of the system using,

$$m_i \ddot{u}_i = \nabla\phi(x_i, y_i, z_i, t) + \sum_{j \neq i} \frac{e^2}{4\pi\varepsilon_0} \frac{1}{(r_i - r_j)^2} \qquad \text{(A.1)}$$

for the sample ions, and

$$m_i \ddot{u}_i = \nabla\phi(x_i, y_i, z_i, t) + \sum_{j \neq i} \frac{e^2}{4\pi\varepsilon_0} \frac{1}{(r_i - r_j)^2} + F_{laser} \qquad \text{(A.2)}$$

for the laser cooled ions. Here, i and j are ion indices, while u stands for the x,y or z coordinate.

The integration technique that was used in our simulation was the Euler Picard Predictor-Corrector method. This particular method helps the integration converge to the actual state to which the system would converge, if the integration was continuous or carried out analytically. This method propagates the ions using the first order propagation formulas: We will use only the x component to illustrate this result.

$$x_{i,n+1}^{p} = x_{i,n} + v_{i,n}\Delta t \tag{A.3}$$

and

$$v_{i,n+1}^{p} = v_{i,n} - \left.\frac{\partial \phi(x,y,z,t)}{m_i \partial x}\right|_{x_n,y_n,z_n} \Delta t \tag{A.4}$$

Where p stands for the predicted positions and velocities and n stand for the integration step. $x_{i,n}$ and $v_{i,n}$ are set by our initial conditions. Eq. (A.4.) is calculated computationally using the following formula for the sample ions

$$v_{i,n}^{p} = v_{i,n} - \frac{\phi(x_n + dx, y_n, z_n, t) - \phi(x_n, y_n, z_n, t)}{m_{i,s}\, dx}\Delta t \tag{A.5}$$

and

$$v_{i,n}^{p} = v_{i,n} - \left[\frac{\phi(x_n + dx, y_n, z_n, t) - \phi(x_n, y_n, z_n, t)}{m_{i,l}\, dx} - \frac{F_{laser}}{m_{i,l}}\right]\Delta t \tag{A.6}$$

for the laser cooled ions. In our simulation, dx was set to 10^{-12} meters. If we were to use these formulas alone to evolve the system, the integration would begin to diverge after only 2-3 ms of integrated motion. Since we needed to simulate the motion for at least 20-30 ms, these predicted positions and velocities needed to be corrected using the following method, namely, the Euler Picard Predictor -Corrector method.

Quite simply, we repeat the steps we have just gone through, i.e. using the first order propagation equations, but this time we will replace our initial velocity $v_{i,n}$ with the average velocity of our initial velocity and the predicted velocity,

$$\frac{v^{p}_{i,n+1} + v_{i,n}}{2} \tag{A.7}$$

and replace our initial position $x_{i,n}$, by the average position of our initial condition and the predicted position.

$$\frac{x^{p}_{i,n+1} + x_{i,n}}{2} \tag{A.8}$$

The newly corrected position now becomes

$$x^{c}_{i,n} = x_{i,n} + \frac{v_{i,n} + v^{p}_{i,n}}{2}\Delta t \tag{A.9}$$

and our newly corrected velocity becomes

$$v_{i,n+1}^{c} = v_{i,n} - \frac{\partial \phi(x,y,z,t)}{m_i \partial x}\Bigg|_{\frac{x_{i,n+1}^{p}+x_{i,n}}{2}, \frac{y_{i,n+1}^{p}+y_{i,n}}{2}, \frac{z_{i,n+1}^{p}+z_{i,n}}{2}, t=t+\frac{\Delta t}{2}} \Delta t \qquad \text{(A.10)}$$

The following method is described schematically below

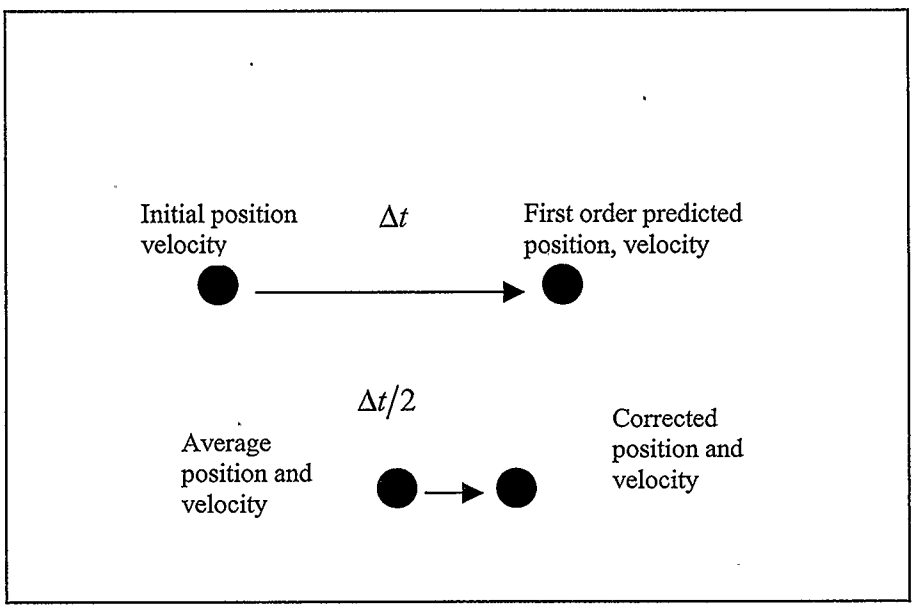

Fig. A1. A schematic diagram showing how the Euler Picard Predictor-Corrector method tackles the problem of divergence during a numerical integration.

Appendix B

C++ Computer code

This computer code provided the basis for my thesis. The code uses the Euler – Picard Predictor-Corrector propagation equations as shown in Appendix A, to simulate the interaction between n_s sample ions and n_l laser cooled ions in a linear quadrupole ion trap environment. The computer output produces a plot of time vs the temperature of laser cooled ions and the temperature of the sample ions. The time steps was generally about 0.1ms depending on the degree of noise. The simulations generally ran for 30-60 ms which corresponded to 2 to 7 days depending on the number of ions (see sections 2.2 and 5.2).

```
#include<fstream.h>
#include<iostream.h>
#include<string>
#include <math.h>
#include <stdlib.h>
int main(void)
{

int p;int x;int i;int j;int o;int y;int n;int set;int g;int sett;int settt;      // Counters
int num,newrand;
double energyion[301];double menergyion[301];      // main particle variables

double xposion[301]; double xvelion[301];
```

```
double yposion[301]; double yvelion[301];
double zposion[301]; double zvelion[301];

double sxposion[301];
double syposion[301];
double szposion[301];

double senergyion[301];                          // Storage particle variables
double nxposion[301]; double sxvelion[301];
double nyposion[301]; double syvelion[301];
double nzposion[301]; double szvelion[301];

                                  // Working variables

double xp;   double yp;   double zp;             // positions
double vxp;  double vyp;  double vzp;            // velocities
double xps;  double yps;  double zps;            // predicted positions
double vxpn; double vypn; double vzpn;           // predicted velocities
double ypsc; double zpsc; double xpsc;           // corrected positions
double vxpc; double vypc; double vzpc;           // corrected velocities
double upnx; double upny; double upnz;           // new potential(x,y,z) for partials
double upn;  double up;   double upm;            // Total Energy variables
double xo;   double yo;   double zo;
double xpsco; double ypsco; double zpsco;
double dvx;  double dvy;  double dvz;            // change in velocities(partials)
double xpm;  double ypm;  double zpm;            // store mid point variables

double prob; double time; double ei; double h; int bin[401];
double waven; double natw; double pl; double satp; double det;
double c; double detmz; double detpz;double detmx; double detpx;
double detmy; double detpy;double nonconz; double nonconx;
double noncony; double counts; double mean; double sigma;
double b; double l; double k; double q; double m; double pi;
double dt; double number; double omega; double voltage;
double energylx; double energyly; double energylz; double energysx;
double energysy; double energysz; double nolci; double output;
double boltz; double outputz;double co; double count;double scatenergy;
double rms,rmsz,rml,rmlz,mlc,msc;int nolcis;double templ;double temps;double rs;
double sfc,sfl,f,templl,tlx,tly,tlz,meanenergy,counttime;

ofstream f1("3p0_40_70_S");                      // Output files
ofstream f2("3p0_40_70_L");
ofstream f3("aaaaasim3.out");
ofstream f4("3p0_40_70");
```

```
ofstream f5("aaasim5.out");
ofstream f6("3p0_40_70_Amp");
//ofstream f7("aaasim7.out");

pi=3.141592654;
dt=0.000000001;                          // constants and trap specifications


voltage=70;                                          // Trapping potential
omega=2.5e6*2*pi*1e-8;  //was 2.90e6  max 8         // Trapping frequency

q=1.6e-19;
l=(q*voltage)/((0.00522/2)*(0.00522/2));
c=3e8; f=80.0;
newrand=2000;
mlc=4.0e-26;                                         // Mass of laser cooled ions
msc=2.0e-26;                                         // Mass of sympathetically cooled ions
nolci=5;                                             // Number of laser cooled ions
k=8.99e9;
waven=2*pi/(280.27e-9);
natw=42.7e6;
pl=6.64e-34/(2*pi);


satp=0.7;
det=-390e6;  //was -390e6

n=1; // output counters


co=0;
number=10;
num=number;
output=10000;
outputz=1000;    // was 200
boltz=1.38e-23;
templ=15;                    // Temperature of laser cooled ions
templl=templ;
temps=40;                    // Temperature of the sympathetically cooled ions
nonconz=0;
nonconx=0;
noncony=0;
counts=0;
```

```
//while(!kbhit()) rand();
x=rand()% newrand;


cout <<"Simulation in progress "<<"\n";
m=mlc;

cout <<"q lc = "<<(2*q*voltage)/(m*1e16*omega*omega*(0.00522/2)*(0.00522/2))<<
"   Secular f lc =
"<<(2*omega*1e8*q*voltage)/(2*pi*m*2.828*1e16*omega*omega*(0.00522/2)*(0.005
22/2))<<" Hz"<<"\n";

sfl=(2*omega*1e8*q*voltage)/(2*pi*m*2.828*1e16*omega*omega*(0.00522/2)*(0.005
22/2));
sfl=sfl*2*pi;

m=msc;
cout<<"\n";
cout <<"q sc = "<<(2*q*voltage)/(m*1e16*omega*omega*(0.00522/2)*(0.00522/2))<<
"   Secular f sc =
"<<(2*omega*1e8*q*voltage)/(2*pi*m*2.828*1e16*omega*omega*(0.00522/2)*(0.005
22/2))<<" Hz"<<"\n";

sfc=(2*omega*1e8*q*voltage)/(2*pi*m*2.828*1e16*omega*omega*(0.00522/2)*(0.005
22/2));
sfc=sfc*2*pi;

time=0;  set=0;   sett=0;
xp=0;   yp=0;    zp=0;
vxp=0;  vyp=0;   vzp=0;
xps=0;  yps=0;   zps=0;
vxpn=0;  vypn=0;  vzpn=0;
ypsc=0;  zpsc=0;  xpsc=0;
vxpc=0;  vypc=0;  vzpc=0;
upnx=0;  upny=0;  upnz=0;
upn=0;  up=0;    upm=0;
xo=0;   yo=0;    zo=0;
xpsco=0; ypsco=0;  zpsco=0;
dvx=0;  dvy=0;   dvz=0;
xpm=0;  ypm=0;   zpm=0;
g=0;    settt=0;  rmsz=0;
rms=0;  rmlz=0;  meanenergy=1;
rml=0;  counttime=1;
```

```
m=mlc;

for(i=1; i<=number; i++)          // Assign particles initial velocities and positions

{

if (i>nolci)
{
m=msc;
templ=temps;
sfl=sfc;
}

x=rand()%400;   //200
h=x*0.000001+0.0248; //0.024
zposion[i]=h;

x=rand()%40;
ei=(boltz*templ/100)*(80+x);
xposion[i]=0.1e-6;
xvelion[i]=sqrt(2*ei/m);
x=rand()%100;
if (x<=49) xvelion[i]=-1*xvelion[i];



x=rand()%40;
ei=(boltz*templ/100)*(80+x);
yposion[i]=sqrt(ei/(sfl*sfl*m/2));
x=rand()%100;
if (x<=49) yposion[i]=-1*yposion[i];

yvelion[i]=0.001 ;

x=rand()%60;
ei=(boltz*templ/100)*(70+x);
zvelion[i]=sqrt(2*ei/m);
x=rand()%100;
if (x<=49) zvelion[i]=-1*zvelion[i];

}
```

// Calculates potential of each ion

```
for(p=1; p<=number ; p++)
{
xp=xposion[p];
yp=yposion[p];
zp=zposion[p];
for(i=1; i<=number; i++)
{
if (i==p) goto tom;

xo=xposion[i];
yo=yposion[i];
zo=zposion[i];

up=up+(k*q*q)/sqrt(((xp-xo)*(xp-xo))+((yp-yo)*(yp-yo))+((zp-zo)*(zp-zo)));
tom:
x=0;
}


up=up-0.5*1*xp*xp+0.5*1*yp*yp+(zp-0.025)*(zp-0.025)*f*1000*q;


energyion[p]=up;
up=0;
}

counts=0; energylx=0; energyly=0; energylz=0;
counts=0; energysx=0; energysy=0; energysz=0;


// ********** Start main prog **********

while (time<=90000000)  //          Time unit step = 1e-8s
{


if (time>=(outputz*co))
{
f3<<"\n"<<time/100000.0<<" ";
//f7 << "\n";
//
}
```

```
if (time >= (output*n))                    // Output Velocity Distribution
{
if (n==1) goto jimmy;


cout <<time/100000.0<<" ms"<<"\n";


f1 << (time/100000.0) <<" "<<((1/(output*1e-8))*energysx)/(number-nolci)<<"
"<<((1/(output*1e-8))*energysy)/(number-nolci)<<" "<<((1/(output*1e-
8))*energysz)/(number-nolci)<<"\n";          // output temp

//cout<<energylx<<" "<<energyly<<"\n";
f2<< (time/100000.0) <<" "<<((1/(output*1e-8))*energylx)/nolci<<" "<<((1/(output*1e-
8))*energyly)/nolci<<" "<<((1/(output*1e-8))*energylz)/nolci<<"\n";          // output
temp
//cout<< ((1/(output*1e-8))*energylx)/nolci<<" "<<((1/(output*1e-
8))*energyly/nolci)<<"\n";
//cin >>x;
//f5 << (time/100000.0) <<" "<<((1/(output*1e-8))*energylz)/nolci<<"
"<<((1/(output*1e-8))*energylx)/nolci<<" "<<((1/(output*1e-8))*energysz)/(number-
nolci)<<" "<<det/1e6<<" "<<(sqrt(counts*counts)/(1e6*output*1e-8))<<"\n";          //
output temp


f4<< (time/100000.0) <<" "<<(2/(5*boltz*output*1e-
8))*q*(energylx+energyly+energylz)/nolci<<" "<<(2/(5*boltz*output*1e-
8))*q*(energysx+energysy+energysz)/(number-nolci)<<"\n";

f6 <<(time/100000.0)<<" "<<((rml)/(output*1e-8))/(1e-6)<<" "<<((rms)/(output*1e-
8))/(1e-6)<<"\n";

tlx=(1/(1*boltz*output*1e-8))*q*(energylx)/nolci;//new laser cooling
tly=(1/(1*boltz*output*1e-8))*q*(energyly)/nolci;//new laser cooling
tlz=(2/(1*boltz*output*1e-8))*q*(energylz)/nolci;//new laser cooling
jimmy:
counts=0; energylx=0; energyly=0; energylz=0; energysx=0; energysy=0; energysz=0;
rms=0;rmsz=0;rml=0;rmlz=0;n=n+1;
}


dt=1e-9;
```

```
start:
upnx=0;upny=0;upn=0;upnz=0;up=0;upm=0;


for(p=1;p<=number;p++)          // ----- Moves one ion, 'p' -------
{

m=mlc;
if (p>nolci) m=msc;



up=energyion[p];                // Transfer main variables into working variables
xp=xposion[p];vxp=xvelion[p];
yp=yposion[p];vyp=yvelion[p];
zp=zposion[p];vzp=zvelion[p];




                                // Propagate particle p

xps=xp+vxp*dt;
yps=yp+vyp*dt;
zps=zp+vzp*dt;



                        // Partial derivative at the initial point

for(j=1;j<=number;j++)          // Coulomb force calculation
{

if (j==p) goto james;

xo=xposion[j];
yo=yposion[j];
zo=zposion[j];

upnx=upnx+((k*q*q)/sqrt(((xp+1e-12-xo)*(xp+1e-12-xo))+((yp-yo)*(yp-yo))+((zp-
zo)*(zp-zo))));
```

```
upny=upny+((k*q*q)/sqrt(((xp-xo)*(xp-xo))+((yp+1e-12-yo)*(yp+1e-12-yo))+((zp-
zo)*(zp-zo))));
upnz=upnz+((k*q*q)/sqrt(((xp-xo)*(xp-xo))+((yp-yo)*(yp-yo))+((zp+1e-12-zo)*(zp+1e-
12-zo))));

james:
x=0;
}
                    // Trap force calculation

upnx=upnx-(0.5*l*cos(omega*time)*(xp+1e-12)*(xp+1e-
12))+(0.5*l*cos(omega*time)*yp*yp)+(zp-0.025)*(zp-0.025)*f*1000*q;
upny=upny+(0.5*l*cos(omega*time)*(yp+1e-12)*(yp+1e-12))-
(0.5*cos(omega*time)*l*xp*xp)+(zp-0.025)*(zp-0.025)*f*1000*q;
upnz=upnz-(0.5*cos(omega*time)*l*xp*xp)+(0.5*cos(omega*time)*l*yp*yp)+((zp+1e-
12)-0.025)*((zp+1e-12)-0.025)*f*1000*q;


//detp=det+waven*vzp/(2*pi);//2*pi*c*waven*(sqrt( (1+(vzp/c)) /(1-(vzp/c)) )-1);
//detm=det-waven*vzp/(2*pi);//2*pi*c*waven*(sqrt( (1-(vzp/c)) /(1+(vzp/c)) )-1);
//cout <<vzp<<" "<<detp<<" "<<detm<<" ";

//noncon=(dt/m)*(pl*waven*natw*2*pi*satp/2)*(1/(1+satp+(2*detm/natw)*(2*detm/nat
w))- 1/(1+satp+(2*detp/natw)*(2*detp/natw)));

dvx=-((upnx-up)*dt)/(m*(1e-12));          // Evaluate partial derivitives
vxpn=vxp+dvx;

dvy=-((upny-up)*dt)/(m*(1e-12));
vypn=vyp+dvy;

dvz=-((upnz-up)*dt)/(m*(1e-12));//+ noncon;
vzpn=vzp+dvz;



if ((sqrt(dvz*dvz)>30) || (sqrt(dvx*dvx)>30) || (sqrt(dvy*dvy)>30))
{
if (sett==1) goto go;
dt=1e-10;
set=1;sett=1;
goto start;
go:
x=0;
```

```
}


xpsc=xp+(vxpn+vxp)*dt/2;
ypsc=yp+(vypn+vyp)*dt/2;
zpsc=zp+(vzpn+vzp)*dt/2;

sxposion[p]=xps; nxposion[p]=xpsc;          // Store variables untill all
syposion[p]=yps; nyposion[p]=ypsc;          // particles have been propagated
szposion[p]=zps; nzposion[p]=zpsc;          // using old infomation.

upnx=0;upny=0;upnz=0;upm=0;up=0;upn=0;

}                    // ******** end move one ion *******

                        //          Eular picard Correction

for(p=1; p<=number ; p++)          // Evaluate new potential of each ion at half way
{                                  // and total potential at the new point

xpm=(sxposion[p]+xposion[p])/2;
ypm=(syposion[p]+yposion[p])/2;
zpm=(szposion[p]+zposion[p])/2;
xpsc=nxposion[p];
ypsc=nyposion[p];
zpsc=nzposion[p];


for(i=1; i<=number; i++)
{
if (i==p) goto jim;

xo=(sxposion[i]+xposion[i])/2;
yo=(syposion[i]+yposion[i])/2;
zo=(szposion[i]+zposion[i])/2;

xpsco=nxposion[i];
ypsco=nyposion[i];
zpsco=nzposion[i];

upn=upn+(k*q*q)/sqrt(((xpm-xo)*(xpm-xo))+((ypm-yo)*(ypm-yo))+((zpm-zo)*(zpm-
zo)));
up=up+(k*q*q)/sqrt(((xpsc-xpsco)*(xpsc-xpsco))+((ypsc-ypsco)*(ypsc-ypsco))+((zpsc-
zpsco)*(zpsc-zpsco)));
```

```
jim:
x=0;
}

upn=upn-(0.5*1*cos(omega*(time+dt/2e-8))*xpm*xpm)+(0.5*cos(omega*(time+dt/2e-
8))*1*ypm*ypm)+(zpm-0.025)*(zpm-0.025)*f*1000*q;
up=up-(0.5*cos(omega*(time+dt/1e-8))*1*xpsc*xpsc)+(0.5*cos(omega*(time+dt/1e-
8))*1*ypsc*ypsc)+(zpsc-0.025)*(zpsc-0.025)*f*1000*q;
menergyion[p]=upn;
energyion[p]=up;
upn=0;
up=0;
}


for (p=1;p<=number;p++)                    // Calculate derivative half way
{

m=mlc;
if (p>nolci) m=msc;

vxp=xvelion[p];
vyp=yvelion[p];
vzp=zvelion[p];

upm=menergyion[p];
xpm=((sxposion[p]+xposion[p])/2);
ypm=((syposion[p]+yposion[p])/2);
zpm=((szposion[p]+zposion[p])/2);

for(j=1;j<=number;j++)   // Coulomb forces calculation part two half way
{
if (j==p) goto fred;

xo=((sxposion[j]+xposion[j])/2);
yo=((syposion[j]+yposion[j])/2);
zo=((szposion[j]+zposion[j])/2);

upnx=upnx+((k*q*q)/sqrt(((xpm+1e-12-xo)*(xpm+1e-12-xo))+((ypm-yo)*(ypm-
yo))+((zpm-zo)*(zpm-zo))));
upny=upny+((k*q*q)/sqrt(((xpm-xo)*(xpm-xo))+((ypm+1e-12-yo)*(ypm+1e-12-
yo))+((zpm-zo)*(zpm-zo))));
```

```
upnz=upnz+((k*q*q)/sqrt(((xpm-xo)*(xpm-xo))+((ypm-yo)*(ypm-yo))+((zpm+1e-12-
zo)*(zpm+1e-12-zo))));


fred:
 x=0;
}
```

// Trap forces calculation

```
upnx=upnx-(0.5*cos(omega*(time+dt/2e-8))*l*(xpm+1e-12)*(xpm+1e-
12))+(0.5*cos(omega*(time+dt/2e-8))*l*ypm*ypm)+(zpm-0.025)*(zpm-
0.025)*f*1000*q;
upny=upny+(0.5*cos(omega*(time+dt/2e-8))*l*(ypm+1e-12)*(ypm+1e-12))-
(0.5*cos(omega*(time+dt/2e-8))*l*xpm*xpm)+(zpm-0.025)*(zpm-0.025)*f*1000*q;
upnz=upnz-(0.5*cos(omega*(time+dt/2e-
8))*l*xpm*xpm)+(0.5*cos(omega*(time+dt/2e-8))*l*ypm*ypm)+((zpm+1e-12)-
0.025)*((zpm+1e-12)-0.025)*f*1000*q;
```

// Laser cooling force calculation

```
detpz=det+waven*vzp/(2*pi);//2*pi*c*waven*(sqrt( (1+(vzp/c)) /(1-(vzp/c)) )-1);
detmz=det-waven*vzp/(2*pi);//2*pi*c*waven*(sqrt( (1-(vzp/c)) /(1+(vzp/c)) )-1);


detpx=det+waven*vxp/(2*pi);//2*pi*c*waven*(sqrt( (1+(vzp/c)) /(1-(vzp/c)) )-1);
detmx=det-waven*vxp/(2*pi);//2*pi*c*waven*(sqrt( (1-(vzp/c)) /(1+(vzp/c)) )-1);

detpy=det+waven*vyp/(2*pi);//2*pi*c*waven*(sqrt( (1+(vzp/c)) /(1-(vzp/c)) )-1);
detmy=det-waven*vyp/(2*pi);//2*pi*c*waven*(sqrt( (1-(vzp/c)) /(1+(vzp/c)) )-1);
//cout << vzp<<" "<<detpz<<" "<<detmz<<" ";

noncony=(dt/m)*(pl*waven*natw*satp/2)*(1/(1+satp+(2*detmy/natw)*(2*detmy/natw))
- 1/(1+satp+(2*detpy/natw)*(2*detpy/natw)));

nonconx=(dt/m)*(pl*waven*natw*satp/2)*(1/(1+satp+(2*detmx/natw)*(2*detmx/natw))
- 1/(1+satp+(2*detpx/natw)*(2*detpx/natw)));

nonconz=(dt/m)*(pl*waven*natw*satp/2)*(1/(1+satp+(2*detmz/natw)*(2*detmz/natw))-
1/(1+satp+(2*detpz/natw)*(2*detpz/natw)));


count=(m*(sqrt(nonconz*nonconz)+sqrt(noncony*noncony)+sqrt(nonconx*nonconx)))/(
pl*3*waven);
```

```
counts=counts+(m*sqrt(nonconz*nonconz))/(pl*waven);   // count rate*dt


dvx=-((upnx-upm)*dt)/(m*(1e-12));        // Evaluate partial derivatives
vxpc=vxp+dvx;

dvy=-((upny-upm)*dt)/(m*(1e-12));
vypc=vyp+dvy;

dvz=-((upnz-upm)*dt)/(m*(1e-12));
vzpc=vzp+dvz;

x= 1+rand()%(num-1);

rs=xvelion[x]/sqrt(xvelion[x]*xvelion[x]);

if ((p<=nolci)  && (tlx>templl))          // laser cooloing and heating prog
{
vxpc=vxpc+1*nonconx;
count=0;
}

if ((p<=nolci)  && (tly>templl))          // laser cooloing and heating prog
{
vypc=vypc+1*noncony;
count=0;
}

if ((p<=nolci)  && (tlz>templl))          // laser cooloing and heating prog
{
vzpc=vzpc+1*nonconz;
count=0;
}


upnx=0;upny=0;upnz=0;upn=0; upm=0;

sxvelion[p]=vxpc;
syvelion[p]=vypc;
szvelion[p]=vzpc;


if ((p<=1) && (time>=(outputz*co)))          // Output positions and velocities
```

```
{
f3<<xposion[p]*1e6<<" "<<yposion[p]*1e6<<" ";
counttime=0;
meanenergy=0;
}

// Set temp variable to zero

}                              // ---------- end move one ion --------


for(i=1; i<=nolci; i++)
{
                              // Transfer new info to main variables for laser cooled ions
xposion[i]=nxposion[i];
yposion[i]=nyposion[i];
zposion[i]=nzposion[i];
xvelion[i]=sxvelion[i];
yvelion[i]=syvelion[i];
zvelion[i]=szvelion[i];
m=mlc;

energylx=energylx + dt*(0.5*m*xvelion[i]*xvelion[i])/q;
energyly=energyly + dt*(0.5*m*yvelion[i]*yvelion[i])/q;
energylz=energylz + dt*(0.5*m*zvelion[i]*zvelion[i])/q;

rml=rml+dt*sqrt((xposion[i]*xposion[i])+(yposion[i]*yposion[i]))/nolci;
rmlz=rmlz+dt*(zposion[i]-0.025)*(zposion[i]-0.025)/nolci;


}


for(i=nolci+1; i<=number; i++)
{
                  // Transfer new info to main variables for sample ions
xposion[i]=nxposion[i];
yposion[i]=nyposion[i];
zposion[i]=nzposion[i];
xvelion[i]=sxvelion[i];
yvelion[i]=syvelion[i];
zvelion[i]=szvelion[i];
m=msc;
energysx=energysx + dt*(0.5*m*xvelion[i]*xvelion[i])/q;
```

```
energysy=energysy + dt*(0.5*m*yvelion[i]*yvelion[i])/q;
energysz=energysz + dt*(0.5*m*zvelion[i]*zvelion[i])/q;

rms=rms+dt*sqrt((xposion[i]*xposion[i])+(yposion[i]*yposion[i]))/(number-nolci);
rmsz=rmsz+dt*(zposion[i]-0.025)*(zposion[i]-0.025)/(number-nolci);

}



if(time>=(outputz*co))
{
co=co+1;
}

time=time+(dt/1e-8);
set=0;sett=0;settt=0;
} // ********** end main prog  **********


return(0);
}
```